Received August 28, 2014, accepted September 15, 2014, date of publication October 23, 2014, date of current version November 5, 2014.

Digital Object Identifier 10.1109/ACCESS.2014.2364234

Backpacking: Energy-Efficient Deployment of Heterogeneous Radios in Multi-Radio High-Data-Rate Wireless Sensor Networks

A. B. M. ALIM AL ISLAM[1], MOHAMMAD SAJJAD HOSSAIN[2], VIJAY RAGHUNATHAN[3], AND YU CHARLIE HU[3], (Senior Member, IEEE)

[1]Department of Computer Science and Engineering, Bangladesh University of Engineering and Technology, Dhaka 1000, Bangladesh
[2]Google Inc., Mountain View, CA 94043, USA
[3]School of Electrical and Computer Engineering, Purdue University, West Lafayette, IN 47907, USA

Corresponding author: A. B. M. Alim Al Islam (razi_bd@yahoo.com)

ABSTRACT The early success of wireless sensor networks has led to a new generation of increasingly sophisticated sensor network applications, such as HP's CeNSE. These applications demand high network throughput that easily exceeds the capability of the low-power 802.15.4 radios most commonly used in today's sensor nodes. To address this issue, this paper investigates an energy-efficient approach to supplementing an 802.15.4-based wireless sensor network with high bandwidth, high power, longer range radios, such as 802.11. Exploiting a key observation that the high-bandwidth radio achieves low energy consumption per bit of transmitted data due to its inherent transmission efficiency, we propose a hybrid network architecture that utilizes an optimal density of dual-radio (802.15.4 and 802.11) nodes to augment a sensor network having only 802.15.4 radios. We present a cross-layer mathematical model to calculate this optimal density, which strikes a delicate balance between the low energy consumption per transmitted bit of the high-bandwidth radio and low sleep power of the 802.15.4. Experimental results obtained using a wireless sensor network testbed reveal that our architecture improves the average energy per bit, time elapsed before the first node drains its battery, time elapsed before half of the nodes drain their batteries, and end-to-end delay by significant margins compared with a network having only 802.15.4.

INDEX TERMS Ad hoc networks, cyberspace, radio communication, wireless sensor networks, network topology.

I. INTRODUCTION

Energy scarcity is one of the most prominent obstacles to the mass deployment of sensor networks. It is traditionally believed that the radios used on sensor nodes are usually responsible for most of the energy consumption [1]. As a result, much research effort [2] has been devoted to minimizing radio energy consumption. Since most of the early sensor network applications such as environmental monitoring [3], habitat monitoring [4], landslide detection [5], etc., required only infrequent data transmissions, early work on energy minimization focused on lowering the sleep-mode power consumption of radios. As a result, a number of ultra-low-power IEEE 802.15.4 compliant radio chips are now available commercially [6].

However, as sensor network technology has matured over the past decade, more sophisticated systems and applications have begun to emerge. An example is Hewlett Packard's CeNSE [7], which attempts to build a "planet wide sensing network." One of its applications is to build a sensing system for collecting high-resolution data pertinent to seismic imaging in order to enable exploration of natural gas and oil reservoirs. Besides, acoustic sensing [8], machine health monitoring [9], and AC sensing [10] are a few other applications that fall into this new generation of sensor network applications. A direct consequence of the increased degree of sophistication in the new applications is the demand for much higher network data rates than before.

802.15.4 radios, designed for low sleep-mode power as mentioned above, are not well suited to cope with this demand for high data rates. An alternative choice is to replace all the 802.15.4 radios in a sensor network with high-bandwidth, transmission-efficient radios such as 802.11 [11]. Here, the term *transmission-efficiency* refers to the fact that these radios have lower energy consumption per bit of transmitted data in comparison to 802.15.4 radios. Such transmission-efficient radios, however, typically have high sleep-mode power. Further, the increased range of these radios adversely affects the amount of spatial reuse possible.

Therefore, if the transmission-efficient radios are too densely deployed, the energy benefits (i.e., transmission efficiency) of these radios are lost. Consequently, the network-level energy efficiency with transmission-efficient radios can be even worse than using only 802.15.4 radios in such cases of dense deployment, as confirmed by our analysis (Section III-D and Section IV-C).

In this paper, we make a key observation that there is a delicate balance between the low sleep power with high spatial reuse capability of short-range 802.15.4 radios and the transmission efficiency of high-bandwidth, long-range 802.11 radios [12]. Exploiting this observation, we propose an energy-efficient network architecture, which we term as *Backpacking*. Our proposed architecture judiciously utilizes both types of radios. Here, in addition to the traditional belief that the radios used on sensor nodes are usually responsible for most of the energy consumption [1], we also consider energy consumption by CPUs on sensor nodes due to their considerable energy consumption while operating with high-bandwidth 802.11 radios.

Consequently, we make the following set of contributions in this paper:

- We analyze network-level energy efficiency of the low-sleep-power 802.15.4 radio and the transmission-efficient 802.11 radio, under varying end-to-end distances, data rates, and sensor node densities.
- Utilizing the results of our analysis, we propose a novel energy-efficient network architecture for high-data-rate sensor networks. The architecture exploits both the low-sleep-power 802.15.4 radio to transmit sensed data and the transmission-efficient 802.11 radio to backpack, i.e., to relay, accumulated sensed data towards the base station.
- We present the solution to a key design challenge in our network architecture: what is the optimal deployment density of the transmission-efficient radio? Our solution is based on a cross-layer mathematical model that characterizes the delicate balance between usage of the two different types of radio.
- Finally, we evaluate the energy efficiency of our proposed architecture using experiments on a real testbed. Our results demonstrate that the proposed architecture can improve average energy per bit, the time elapsed before the first node dies, the time elapsed before half of the nodes die, and end-to-end delay by significant margins compared to an architecture that uses only one 802.15.4 radio per node.

II. MOTIVATION AND RELATED WORK

There are a number of research studies on improving throughput [13]–[15], energy efficiency [16], [17], and both of them [18] for wireless sensor networks utilizing only 802.15.4. However, the limited capacity of 802.15.4 makes it inherently suitable for low-data-rate networks. Therefore, the sole utilization of 802.15.4 is not enough for supporting emerging high-data-rate wireless sensor network applications (see Section III for more detail). Consequently, research studies exploiting even multiple 802.15.4s [15] are not suitable for the high-data-rate applications. Note that [15] reports better energy efficiency using multiple 802.15.4s, however, from single-node perspective. The network-level energy efficiency can exhibit a completely different phenomena compared to the single-node perspective. This happens as the network-level energy efficiency considers the impact of transmissions from multiple nodes, which is ignored in the single-node case. Consequently, the network-level energy efficiency can significantly vary depending on different network parameters, whereas the single-node case remains same independent of the network dynamics (see Section III). Another argument on exploiting multiple 802.15.4s [15] not being suitable for the high-data-rate applications is that exploiting multiple 802.15.4s can split the application data over available 802.15.4s to enhance energy efficiency. Such splitting reduces data transmission rate over each available 802.15.4. However, even with such reduction, we cannot achieve any significant improvement from the perspective of *network-level* energy efficiency (see Fig. 4a, where network-level energy efficiency remains almost same even after reducing data transmission rate over 802.15.4 to less than its half value, i.e., from 500 pps to 200 pps). As a result, exploiting heterogeneous radios in wireless sensor networks becomes a necessity rather an ambitious extension of the in situ 802.15.4-based networks.

In recent times, the notion of exploiting heterogeneous radios in wireless sensor networks has been investigated by several research studies for efficient data collection [19]–[21] and for improving network scalability [22], [23]. However, none of these studies focuses on energy efficiency of the network. Some other studies [24]–[28] investigate exploitation of heterogeneous radios mainly focusing on energy efficiency from the perspective of a single sensor node. However, such node-level energy efficiency significantly differs from the network-level energy efficiency. Our thorough illustration on network-level energy efficiency, presented in this paper, clearly depicts the difference.

Besides, a theoretical study [29] on heterogeneous wireless sensor networks proposes Integer Linear Programming based models and heuristic algorithms for optimally deploying gateways in the network. However, this study does not consider impacts of various characteristics of real radios (such as bandwidth, transmission range, etc., which we will present in Section III-A). Moreover, it does not take into account different modes of operations of sensor nodes (such as sleep mode, transmission mode, etc.) while focusing on energy consumption. Consequently, this study can not be applied for optimizing network-level energy efficiency of a real wireless sensor network. Additionally, Siphon [30] exploits the applicability of a long-range radio along with the conventional 802.15.4 in sensor networks to alleviate congestion by escaping the area of congestion using the long range of the additional radio. It mainly considers the reduction in the number of dropped packets by utilizing the additional

long-range radio rather than focusing on energy-efficient deployment of the additional radio. Besides, [21] investigates deployment of dual-channel and dual-band radios for enhancing delivery rates and network scalability. However, this study suggests that such deployment decreases network energy efficiency while enhancing the intended metrics. Therefore, similar to the previous study, this study also ignores the notion of energy-efficient deployment of multiple radios.

In addition, BCP [31] investigates the applicability of 802.11 in a sensor network by deploying them in all sensor nodes. It argues for buffering the sensed data and delaying the transmission of the buffered data to exploit the energy efficiency of 802.11. Here, the notions of buffering and delaying eventually increase the end-to-end delay during the operation. In addition, BCP does not consider the impact of interference resulted from simultaneous data transmission from multiple nodes. However, such impact can adversely affect the network-level energy efficiency while deploying 802.11 at each sensor node, which we confirm through our simulation results presented in Section III-D. Similarly, another study [32] investigates the applicability of Bluetooth radio to all sensor nodes in the network. Nonetheless, both [31] and [32] attempt to exploit a transmission-efficient radio by only considering its high bandwidth. They do not consider the impact of deployment density of the long-range radio, which has the potential to significantly affect network-level energy efficiency even in an adverse way (discussed in Section III-D). Moreover, deployment of transmission-efficient radio to all sensor nodes can significantly degrade network-level energy efficiency of a sensor network (see Section III-D) as sleep mode power of the transmission-efficient radio is very high and even comparable to transmission mode power of 802.15.4 (see Section II-B).

To the best of our knowledge, we [12] are the first to study the impact of deployment density of long-range and high-bandwidth radios, in addition to the impact of their power consumption, transmission range, and bandwidth, to eventually optimize *network-level* energy efficiency of a wireless sensor network experiencing high-data-rate transmission. Besides, we simultaneously consider the impact of transmissions from multiple radios while analyzing the network-level energy efficiency. In this paper, we extend the analysis presented in [12] (see Section III-C, III-D, and IV-C). Besides, in this paper, we present new testbed experiments consisting only sensor nodes (Section V), whereas we have utilized laptops in place of accumulator nodes in [12]. Additionally, in this paper, we investigate the impact of deployment of a higher number of accumulator nodes in the testbed to validate the outcome of our proposed mathematical model, which we did not do in [12]. Finally, we also elaborate applicability of our study in this paper (Section VII), which was not present in [12].

It is worth mentioning that there are a number of studies in the literature on clustering wireless sensor networks [33]–[38] and on judicious deployment of sensor nodes [39]–[41], which exhibit somewhat similar flavor from the high-level while being compared with our study. However, none of these already-available studies focuses on high-data-rate transmission over wireless sensor networks, which we do in our study presented in this paper.

Now, before presenting our study in this paper, we further illustrate the motivation of our work in the following two subsections. First, we elaborate on wireless sensor networks experiencing high-data-rate transmission.

A. HIGH-DATA-RATE TRANSMISSION IN WIRELESS SENSOR NETWORKS

A number of wireless sensor networks are experiencing high-data-rate transmission in recent times. In these networks, the high data rate may arise in two different cases:

1) Due to accumulation of data from a low-data-rate application in a large sensor network,
2) Due to the presence of a high-data-rate application itself.

CeNSE [7], which attempts to build a ''Central Nervous System'' for the Earth by deploying millions of sensor nodes, provides an emerging example corresponding to the first case. Besides, other large-scale sensor networks [42], [43] can also experience high-data-rate transmission within the network in a similar way. In the second case, we can find several recent high-data-rate applications of sensor networks. For example, seismoacoustic monitoring demands a high-data-rate transmission of $\sim$100 packets per second (pps) [44], and thus significantly threatens network lifetime through high power consumption at each sensor node. Structural health monitoring is another prominent example of high-data-rate application of sensor networks [45]–[51], which can involve a data rate of 500 pps [46], [48]. Such networks are already deployed in several places such as in Stanford Earthquake Engineering Center [49], [50] and at Golden Gate Bridge [51]. Another example of high-data-rate sensor network applications is condition-based maintenance [52], [53]. Besides, the sensor networks used for biological monitoring of neural signals also demand high-data-rate transmission ($\sim$100 pps) [54]. In addition, performing acoustic sensing over sensor networks, may demand an even higher rate of data transmission ($\sim$8000 pps) [54]. Finally, some emerging applications of sensor networks such as aerospace applications (for example aircraft testing) [55] also demand high-data-rate transmission.

To summarize, there are numerous cases where wireless sensor networks are experiencing high-data-rate transmission. The data rate may even be increased in future applications. Therefore, we attempt to study a suitable network architecture, exploiting multiple heterogeneous radios, to support such high-data-rate applications over wireless sensor networks.

B. AVAILABLE RADIO ALTERNATIVES FOR SUPPORTING THE HIGH-DATA-RATE TRANSMISSION

State-of-the-art network architecture of wireless sensor networks uses only 802.15.4 radios, and hence is not

capable of supporting high-data-rate applications. Consequently, several research studies such as LEAP [27] and mPlatform [25] attempted to use transmission-efficient radios on sensor nodes. However, these studies mainly focused on developing advanced sensor platforms rather than investigating how to deploy the transmission-efficient radios in a wireless sensor network in an energy-efficient manner. Subsequent studies utilizing transmission-efficient radios [15], [28], [32] analyzed the notion of energy-efficient operation, however, being limited to a single-node perspective rather than exploring the network perspective. Few studies [21], [31] investigated network energy consumption while using transmission-efficient radios at each sensor node. However, these studies did not analyze the notion of *selective* deployment of the transmission-efficient radios, i.e., low density deployment of the radios.

A primary challenge in enhancing the energy efficiency of wireless sensor networks from the network perspective using transmission-efficient radios is how to determine the deployment density of the transmission-efficient radios. The density of deployment determines the number of nodes that are affected by the blackout footprint of a transmitting node. The short transmission range of 802.15.4 radios generally limits the number of such affected nodes to a small value, and hence exhibits meager impact in this regard. However, the long range of transmission-efficient radios results in a larger number of such affected nodes. Therefore, the deployment density exhibits a significant impact in the case of transmission-efficient radios. Moreover, changing the state of the affected nodes to sleep mode would not help either, as the sleep power of the transmission-efficient radios is comparable to the transmission power of 802.15.4 radios [6], [56]. To further analyze such tradeoff, we investigate network-level energy efficiency of different radios in the next section.

III. RADIO ENERGY EFFICIENCY: NETWORK PERSPECTIVE

We start our study by comparing the energy efficiencies of 802.15.4 and 802.11 radios from the network perspective. A previous comparison study [24] was for a single sensor node, which ignores the impact of transmissions from multiple nodes and variation in transmission ranges of the radios. In the following, we study the comparison by separately deploying the radios in varying network settings.

Henceforth, we refer to the transmission-efficient radio, i.e., 802.11, as the *Backpack* radio, as we intend to deploy it in sensor networks to backpack sensed data towards the base station. In addition to 802.11, we also discuss other possibilities for the *Backpack* radio technology in Section VI.

A. DIVERSITY IN ENERGY EFFICIENCIES OF DIFFERENT RADIOS

We compare the energy efficiency of 802.15.4 and a variant of 802.11 (802.11b) considering their power consumption, bandwidths, and transmission ranges. We utilize the measurements provided in [6] and [56] to calculate the power consumption of the radios. We present the power consumption in different modes, transmission ranges, and bandwidths of 802.15.4 (in TelosB [2]) and 802.11b (in Stargate [26]) in Table 1. The associated CPUs with the radios (MSP430 for 802.15.4 and XScale PXA255 for 802.11b) also consume power during their operations. Since the consumption by the CPU for operating the high-bandwidth radio such as 802.11b can be considerable [24], we incorporate the power consumption of the CPU in the power ratings presented in the table. Further, we consider 10% duty cycling in the calculation of the sleep power for both the radios. Here, we adopt the value of duty cycle to be 10% (or equivalently 0.1), as such value has frequently been adopted for wireless sensor networks [57]–[60]. Besides, we do not choose a lower value for duty cycle to better support high-data-rate transmission, which is our focus in this paper. Besides, our consideration of duty cycling leads to taking a weighted sum of original sleep-mode power and idle-mode power as the sleep power in operation. Here, we consider $0.9 \times P_{sleep} + 0.1 \times P_{idle}$ as the sleep power in our study adopting 10% duty cycling, where P_{sleep} is the original sleep-mode power and P_{idle} is the original idle-mode power.

TABLE 1. Power consumption in different modes, transmission ranges, and bandwidths for 802.15.4 and 802.11b radios.

Attribute	802.15.4 radio	802.11b radio
Transmission power (mW)	52.2	1679
Reception power (mW)	59.1	1560
Sleep power (mW)	0.65	41.58
Transmission range (m)	40	250
Bandwidth (Mbps)	0.25	11

Table 1 shows that the transmission, reception, and sleep power of 802.11b are higher than that of 802.15.4 by about 32, 26, and 64 times accordingly. However, the transmission range and bandwidth of 802.11b are higher than that of 802.15.4 by about 6 and 44 times respectively. Therefore, 802.15.4 provides its low power consumption at the expense of a reduced transmission range and small bandwidth. As a consequence, 802.15.4 requires a deployment of more nodes to cover the same area and more transmission time to transmit the same amount of data in comparison to 802.11b. Both of these requirements incur increased energy consumption for 802.15.4. Therefore, the trade-off in deployments of 802.15.4 and 802.11b for optimized energy-efficiency is not obvious. To understand this trade-off, we perform a rigorous experimental analysis to compare the energy efficiencies of 802.15.4 and 802.11b. We perform our experiments using `ns-2` [61] simulations in different network topologies.

B. SIMULATION SETTINGS

We simulate linear and random topologies to gain the insight of energy efficiencies of 802.15.4 and 802.11. In the case of 802.11, we use system attributes pertinent for 802.11b. However, as we mainly focus on the transmission efficiency of 802.11, from now on, we refer to the 802.11b using 802.11 and omit the specific protocol.

In ns-2, the MAC layers associated with 802.15.4 [62] and 802.11 are different. Here, the MAC layer of 802.11 utilizes the notion of RTS and CTS supplementing CSMA/CA, whereas the MAC layer of 802.15.4 omits the notion of RTS and CTS. In the case of 802.15.4, we utilize unslotted CSMA/CA in the MAC layer having default parameters as utilized in the development of 802.15.4 in ns-2 (presented in [62]). We adopt the unslotted CSMA/CA due to its low operational overhead [63]. Now, considering the variation in the MAC layer operations, we also simulate the combination of 802.15.4 radio along with the MAC layer associated with 802.11 to make a fare comparison between the two radios irrespective the operations of the MAC layers. We term this combination as the "802.15.4+RTS/CTS."

We utilize the measurements presented in Table 1 along with the radio startup power in our simulation. In the simulation, we utilize an updated energy module of ns-2 [64] to compute energy consumption of sensor nodes while operating with duty cycling. Besides, we consider an application payload of 64 bytes in each packet transmitted from a sender node. Here, we adopt the Two-Ray Ground Reflection model [65] as the wave propagation model in the transmission of the packets. In addition, we use a drop-tail, priority queue having a capacity of 50 packets in each node for buffering the packets intended for transmission. Finally, we use UDP as the transport layer protocol and DSDV [66] as the routing protocol to enable transmissions over loop-free, minimum-hop paths. It is worth mentioning that we have utilized UDP and DSDV in our simulation due to the availability of their corresponding modules in ns-2. Other protocols, which are more common in the case of wireless sensor networks [36], [67], could be used in this regard. Nonetheless, we argue that simulation with any of these protocols will eventually lead to similar *relative* results for different radio alternatives in our study, as our study mainly focuses on the radio capabilities rather exploiting the efficiency of the higher-layer protocols.

C. ANALYSIS IN THE LINEAR TOPOLOGY

We start our analysis in a simple linear topology. We use one source-destination pair placed at two ends of the topology to evaluate the performance of 802.15.4 and 802.11. We separately vary the distance between the source-destination pair and the data rate at the source node. The motivation behind varying the distance is to study the impact of deploying an increased number of nodes with 802.15.4 than with 802.11 to cover increasingly large distances. The reasons behind the impact are twofold. First, the increased number of nodes with 802.15.4 increases the total energy consumption. In addition, it also increases the number of hops, which decreases the network throughput. On the other hand, we vary the data rate to reveal the phenomena that occur when the data rate exceeds the capacity of 802.15.4 while remaining within that of 802.11.

First, we vary the distance between the source-destination pair from 60m to 150m. We place the nodes with 802.15.4 30m apart from the adjacent nodes to cover the varying distance. Therefore, an increase in distance by 30m implies an increase in the number of hops by 1 when using 802.15.4. On the other hand, we place only two nodes with 802.11 to cover up to 150m distance in between them. In both cases, we consider that the source node transmits at the rate of 1000 packets per second (pps) to the destination node.

It is worth mentioning that we do not consider any denser deployment with 802.15.4, as such denser deployment would result in worse network performance in presence of high-data-rate transmission. For example, we simulate the case with 60m distance between the source-destination pair considering two denser deployments by setting the distance between two adjacent nodes to 20m and 15m respectively. In both the cases, network throughput decreases and total energy consumption increases compared to that we get with 30m distance between two adjacent nodes. Consequently, we find 2 times and 5237 times increased average energy per bit in these two settings respectively compared to that we get with 30m distance. Here, the menacing increase of 5237 times in the case of 15m distance is due to ending up with a very small network throughput. This outcome contradicts the intuitive increasing change [68] on throughput with a decrease in the distance between two adjacent nodes. This contradiction happens in our simulation due to high rate in data transmission. Such high-data-rate transmission significantly increases the extent of interference in a denser topology due to having a larger number of transmitting nodes within the interference rage of a node.

In addition, note that we perform our simulation up to the distance of 150m between the source-destination pair. We have not presented results beyond that distance as such increase significantly decreases network throughput over the settings with 802.15.4. Here, the network throughput completely diminishes in case of 210m and 240m distances over the networks with 802.15.4 and 802.15.4+RTS/CTS respectively.

Now, we present our simulation results. Fig. 1 shows the impact of variation in the distance between the source and destination nodes. Fig. 1a depicts that after a certain distance (90m), using 802.11 consumes less average energy per transmitted bit than using 802.15.4 and using 802.15.4+RTS/CTS. This occurs due to the decrease in throughput (Fig. 1b) and increase in total energy consumption (Fig. 1c) in the later two cases, whereas both the throughput and total energy consumption remain the same for 802.11 in response to the increase in the distance. Here, the decrease in throughput results from the decrease in packet delivery ratio due to an increase in the number of hops, which we depict in Fig. 1d. Further, using 802.11 exhibits significantly smaller end-to-end delay (Fig. 1e) due to its single-hop and high-bandwidth transmission.

Second, we place the source and destination nodes at a distance of 120m apart to analyze the impact of variation in data rates. The results, shown in Fig. 2a, suggest that using 802.11 consumes less average energy per bit than both

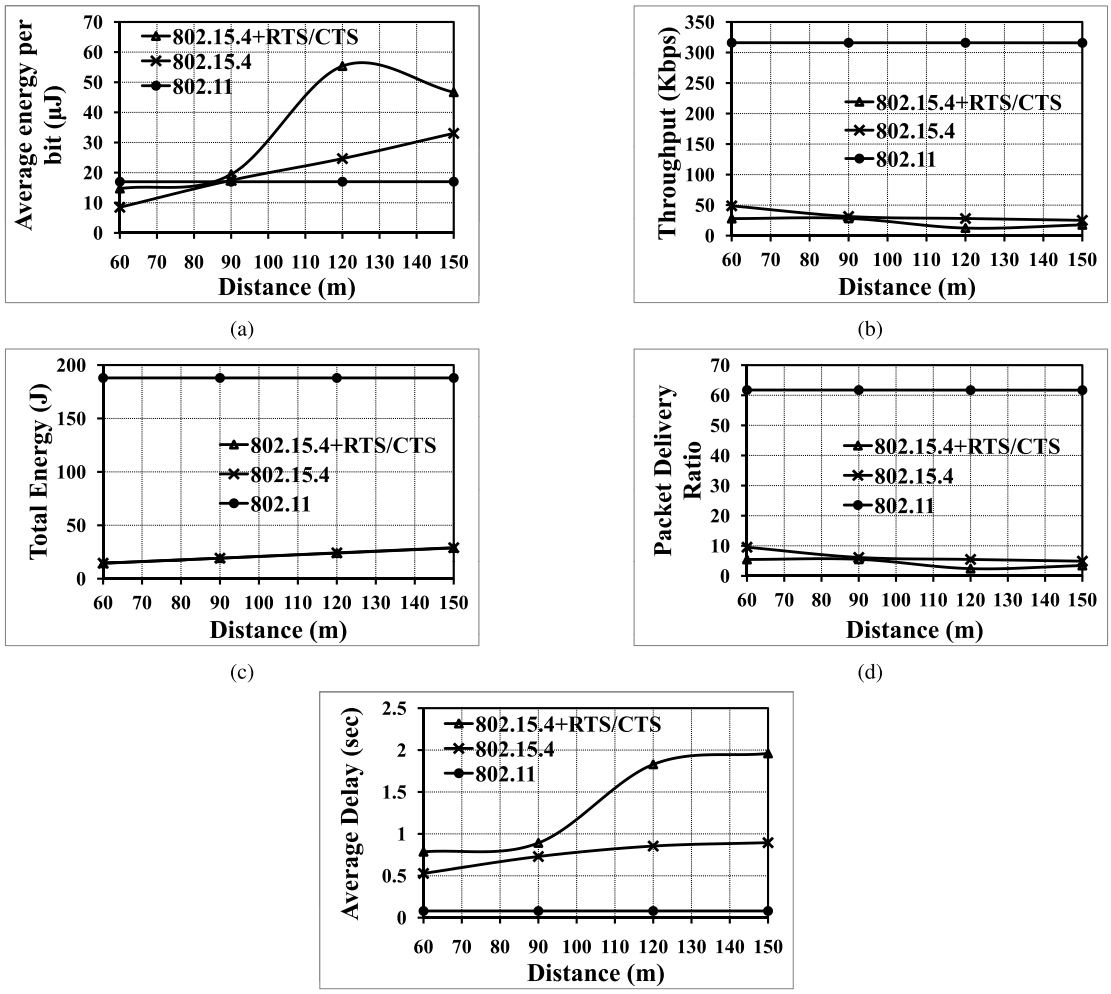

FIGURE 1. Impact of variation in end-to-end distance. (a) Average energy per bit. (b) Total network throughput. (c) Total energy consumption. (d) Delivery ratio. (e) Average end-to-end delay.

using 802.15.4 and using 802.15.4+RTS/CTS after a certain data rate (400 pps). This occurs due to the faster increase in throughput than that in total energy consumption in the case of 802.11, whereas both throughput and total energy consumption remain at almost constant values for 802.15.4 in response to the increase in the data rate. Fig. 2b and Fig. 2c show the trends in throughput and total energy consumption respectively. Here, the fast increasing trend in throughput of 802.11 results from the fast increasing phenomena in its packet delivery ratio, which we depict in Fig. 2d. Besides, similar to the case of variation in distance, 802.11 again exhibits significantly smaller end-to-end delay (Fig. 2e) for all the data rates due to its single-hop and high-bandwidth transmission.

In Fig. 1 and Fig. 2, 802.15.4+RTS/CTS exhibits a bit fluctuating performance with the increases in distance and data rate due to varying impact of the hidden stations. However, even with the fluctuation, it performs worse than 802.15.4 in most of the cases due to the overhead involved with RTS/CTS.

Besides, it is worth mentioning that we attempt to show the difference in the capabilities of two radios, 802.15.4 and 802.11, even under similar MAC in Fig. 1 and Fig. 2. Here, the bottleneck in the case of worse performance with 802.15.4 is the shorter transmission range and low bandwidth of 802.15.4 rather the operation of any higher layer such as the corresponding MAC layer. This becomes evident through analyzing the performance of 802.15.4 with two different variants of MAC. Here, even in the presence of CSMA MAC excluding RTS/CTS, which is the more suitable option for 802.15.4 [62], the performance with 802.15.4 is significantly worse compared to that of 802.11. Consequently, we argue that our motivation, based on the results presented in this section, holds irrespective of utilizing different variants of higher layers (such as MAC) with 802.15.4.

D. ANALYSIS IN THE RANDOM TOPOLOGY

To gain further insight into the impact of the long transmission range of 802.11, we perform simulation in a random topology. We simulate several random topologies

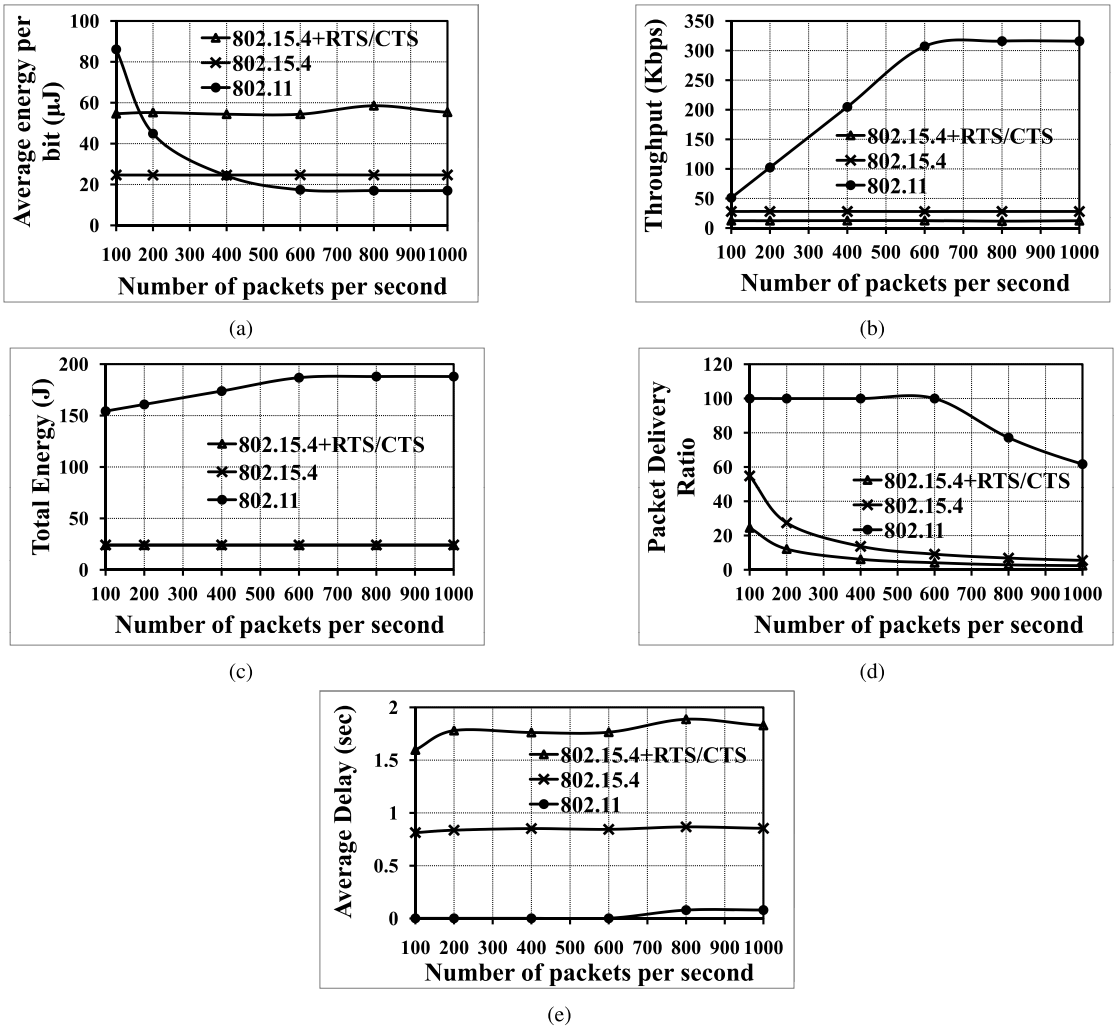

FIGURE 2. Impact of variation in data transmission rate. (a) Average energy per bit. (b) Total network throughput. (c) Total energy consumption. (d) Delivery ratio. (e) Average end-to-end delay.

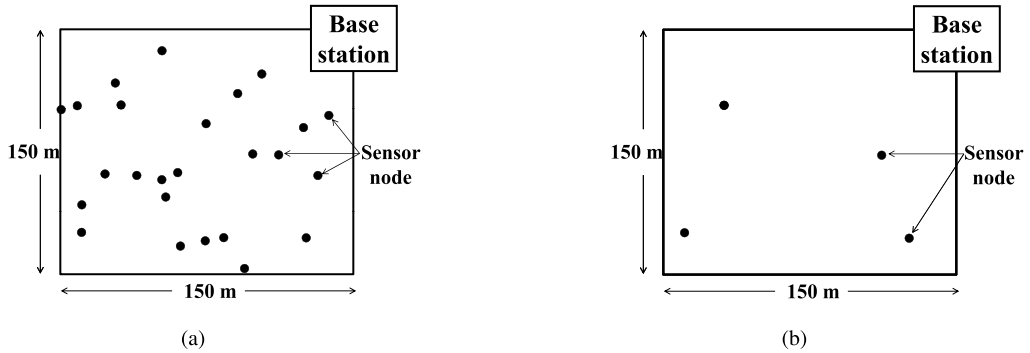

FIGURE 3. Example scenarios of random node placement over a coverage area of 150 × 150m^2 having a cornered base station. (a) Random placement of 25 nodes. (b) Random placement of 4 nodes.

over a coverage area of 150 × 150m^2 having a base station at (150m, 150m), i.e., at a corner of the coverage area. Here, we compare four different deployment scenarios. In the first two scenarios, we randomly place 25 nodes with 802.15.4 and 802.15.4+RTS/CTS, respectively, over the coverage area in two separate settings. In the last two scenarios, we place 25 and 4 nodes with 802.11 in two other separate settings, respectively, to analyze the impact of high and low density 802.11 deployments accordingly. The average number of neighbor nodes is 3 in the settings with 802.15.4, 802.15.4+RTS/CTS, and low density 802.11, and 24 for the setting with high density 802.11. Fig. 3 shows two examples

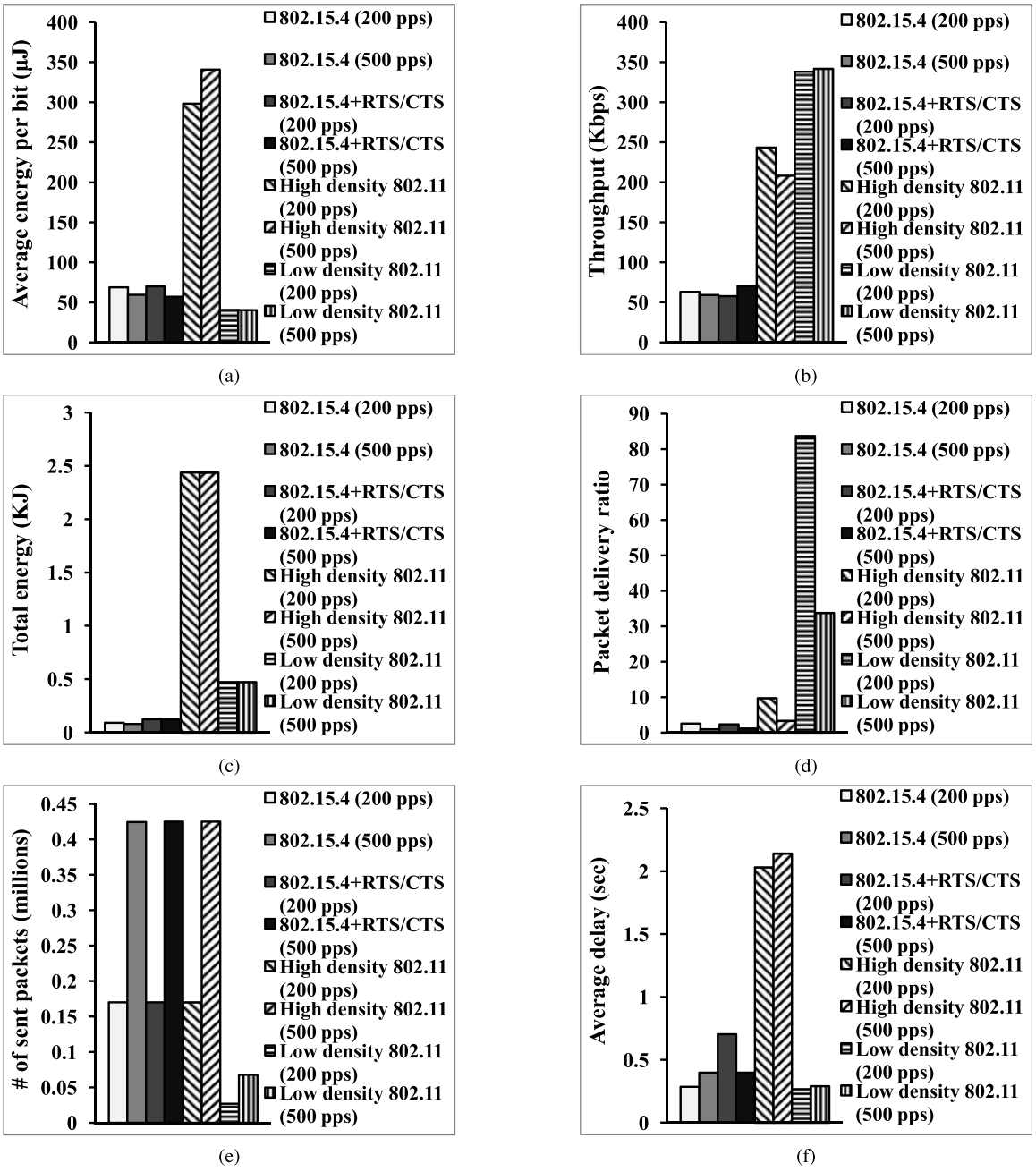

FIGURE 4. Performance comparison in random topologies over an area of 150 × 150m^2. (a) Average energy consumption per bit. (b) Total network throughput. (c) Total energy consumption. (d) Delivery ratio. (e) Number of sent packets. (f) Average end-to-end delay.

of random node placement with 25 (Fig. 3a) and 4 (Fig. 3b) nodes.

In all cases with random node placement, we enable simultaneous data transmissions from all nodes toward the base station at two different data rates, 200 pps and 500 pps, to ensure that the trend in the simulation results is independent of the changes in data rates. With these network settings, we take the average of five simulation runs and present the results in Fig. 4.

Using 802.15.4 and using 802.15.4+RTS/CTS exhibit similar values in average energy per bit, total network throughput, and total energy consumption. However, the end-to-end delay using 802.15.4+RTS/CTS is higher than that of using 802.15.4 due to the overhead of RTS/CTS. Therefore, from now on we focus on 802.15.4, eliminating the notion of RTS/CTS with it.

On the other hand, 802.11 radio exhibits significantly varying performance for different densities in the random topology. Irrespective of the variation in density, using 802.11 always exhibits higher throughput (Fig. 4b) than that using 802.15.4 due to the higher bandwidth of 802.11 in comparison to 802.15.4. The phenomenon of this higher

throughput results from a combined effect of packet delivery ratio (Fig. 4d) and number of sent packets (Fig. 4e). Either of these two outcomes is significantly higher in the case of 802.11. Consequently, their product, i.e., throughput, becomes higher in this case compared to that using 802.15.4.

Nevertheless, we achieve lower network throughput in the high density 802.11 setting than in the low density setting. This results from the high extent of interference with 802.11. The reason behind the high extent is the longer transmission range of 802.11, which eventually results in a larger interference region. The larger interference region shows significant impact even though we use RTS/CTS.

In the presence of the larger interference region, RTS/CTS itself becomes highly prone to interference. We get an essence of this phenomena by analyzing Fig. 4e. Here, the high density setting sends 6.27 times the packets compared to low density setting. However, the increase in the number of nodes is 4.25 times, and all nodes transmit data at the same speed. Moreover, for both the settings, each node is within interference regions of all other nodes and thus should observe RTS/CTS from other nodes in a similar way. Therefore, the expected increase in the number of sent packets should not exceed 4.25 times. Here, the unexpected increase, i.e., the increase by 6.27 times going beyond 4.25 times, arises from significant losses of RTS/CTS itself due to interference.

Further, the high density setting consumes significantly higher total energy than that in the low density setting (Fig. 4c) due to the sleep energy consumption by 802.11 while being in a blackout period. The combined impact of higher total energy consumption and lower throughput explain the high average energy per bit in the case of a high density setting (Fig. 4a). Besides, the waiting time in the high density setting results in a significant increase in end-to-end delay (Fig. 4f).

We analyze the results of random topologies over an area of $150 \times 150\text{m}^2$ (Fig. 4) in depth to highlight the severe consequence of deploying 802.11 in a high density manner. To further investigate the consequence, in addition to analyzing the capability of 802.15.4, we have also simulated random topologies over an area of $250 \times 250\text{m}^2$. Fig. 5 shows

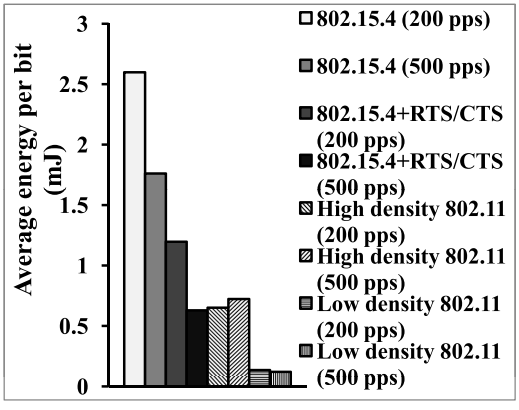

FIGURE 5. Average energy consumption per bit in random topologies over an area of $250 \times 250\text{m}^2$.

average energy consumption per bit in this case. Here, similar to the earlier case, we find the lowest values of energy consumption while using low density 802.11. Besides, this figure reveals that the performance of 802.15.4 gets worse over the larger area of $250 \times 250\text{m}^2$. This happens as the distance between source and destination nodes increases in random topologies over the larger area. Consequently, following the finding of Fig. 1a, i.e., energy consumption per bit increases in case of 802.15.4 with higher values of distance between source and destination nodes, using 802.15.4 results in higher values of energy per bit compared to the previous case over $150 \times 150\text{m}^2$.

To further validate this finding of getting worse performance using 802.15.4 over larger coverage area, we perform similar simulation over an area of $400 \times 400\text{m}^2$. Here, we separately deploy 100 nodes each having one 802.15.4 and 4 nodes each having one 802.11. We increase the number of nodes each having 802.15.4 from 25 to 100 considering the smaller transmission range of the radio. Our simulation results over an area of $400 \times 400\text{m}^2$ demonstrate that using 802.15.4 exhibits 113 times average energy consumption per transmitted bit compared to that found using 802.11. In the earlier case over $250 \times 250\text{m}^2$ area, we have found that using 802.15.4 exhibits 19 times average energy consumption per transmitted bit compared to that found using 802.11. Nonetheless, in the first case (over $150 \times 150\text{m}^2$ area), the same ratio was only 2, i.e., only 2 times average energy consumption per transmitted bit using 802.15.4 compared to that found using 802.11. These results clearly indicate that using 802.15.4 exhibits significantly worse performance over larger coverage areas in case of high-data-rate transmission. This finding reveals incompetence of state-of-the-art network architecture for high-data-rate wireless sensor networks having larger coverage areas. Consequently, this finding points out the significance of using Backpacking architecture with no other alternative for high-data-rate wireless sensor networks having larger coverage areas.

It is worth mentioning that in both the latter cases, i.e., over an area of $250 \times 250\text{m}^2$ and over an area of $400 \times 400\text{m}^2$, we experience multi-hop data transmissions over 802.11.[1] To clarify the multi-hop data transmission, note that the diagonals of the areas are 354m and 566m respectively. Both of these diagonals are greater than the transmission range of 802.11, i.e., 250m, which enforces the multi-hop transmission. Consequently, we can state that findings from our simulation results cover impacts of multi-hop transmissions over both the radios.

Finally, note that the high-density deployments of 802.11 in all the cases also investigate the scenario of deploying 802.11 at each sensor node in place of 802.15.4, i.e., complete replacement of 802.15.4 by 802.11 at each sensor node. All such cases exhibit higher average energy consumption per

[1]Such multi-hop transmissions over 802.11 were absent in the first case while simulating over $150 \times 150\text{m}^2$ area, as the diagonal of this area (212m) is less than the transmission range of 802.11 (250m).

bit compared to that in low-density deployment of 802.11. Therefore, the results suggest that complete replacement of 802.15.4 by 802.11, or inclusion of 802.11 at each sensor node, is not the most energy-efficient solution.

E. SUMMARY OF FINDINGS

We summarize four key findings obtained from our simulation study over the deployments, having different radios in linear and random topologies as follows:

1) Using 802.15.4 consumes higher average energy per bit than using 802.11 above a certain distance between the source and destination sensor nodes of a flow.
2) Using 802.15.4 consumes higher average energy per transmitted bit than using 802.11 above a certain data transmission rate.
3) The high density deployment of 802.11 nullifies the energy efficiency that is achieved due to its high bandwidth.
4) Using 802.11 achieves significantly low average end-to-end delay in low density deployment due to the exploitation of its higher bandwidth and low waiting time as well.

Based on these findings, we design an architecture that makes use of both types of radio in wireless sensor networks.

IV. DESIGN OF AN ENERGY-EFFICIENT ARCHITECTURE

In this section, we propose a hybrid energy-efficient architecture for high-data-rate sensor networks. The architecture utilizes both 802.15.4 and 802.11 radios to exploit all of the key findings revealed in the previous section.

A. ARCHITECTURE

In the proposed architecture, we consider two types of sensor nodes, *originator* and *accumulator*. An originator node only performs sensing tasks. It is equipped with one 802.15.4 to transmit the sensed data over it. However, an accumulator node utilizes an 802.15.4 and an 802.11. It accumulates sensed data from other originator nodes using 802.15.4 and backpacks the accumulated sensed data towards the base station using 802.11. Due to the notion of the *backpack* operation, we term our architecture as *Backpacking*. Fig. 6 presents

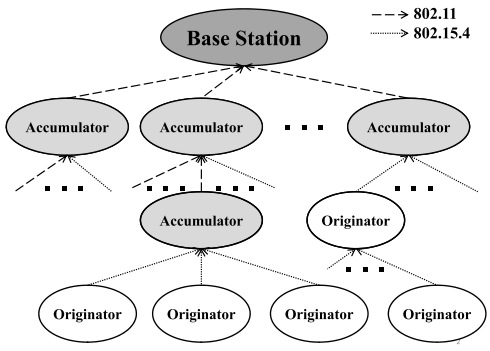

FIGURE 6. Data accumulation at the base station in our proposed Backpacking architecture.

data accumulation at a base station through different types of nodes using different radios in our proposed architecture. The architecture exhibits a flavor of being hierarchical. Note that the accumulator nodes may perform data aggregation before backpacking accumulated data towards the base station over 802.11. However, in the analysis presented in this paper, we have not considered such aggregation. Therefore, in our analysis, the accumulator nodes simply backpacks its accumulated data as they are in an instantaneous manner.

An originator node transmits its sensed data to the nearest accumulator node. We minimize the transmission distance between an originator node and the nearest accumulator node by imposing minimum-hop and loop-free routing over 802.15.4 to exploit the first key finding.

An accumulator node accumulates the sensed data from some originator nodes and transmits that towards the base station. The transmission of such accumulated sensed data follows minimum-hop paths only over 802.11. Here, the data accumulation enables high-data-rate transmission over each 802.11 in the network and thus exploits the second key finding.

Finally, to exploit the third and fourth key findings, we need to find the optimal density of 802.11 in the network. We find the optimal density using a cross-layer mathematical model.

B. MATHEMATICAL MODEL FOR OPTIMAL BACKPACK DENSITY

We consider UDP at the transport layer and minimum-hop routing at the network layer in our formulation. We further consider transmission of RTS/CTS in the case of the MAC for 802.11 and best-effort transmission in the case of the MAC for 802.15.4. Besides, we adopt the RSS-based *Physical Model* [69] for data transmission at the physical layer.

In our work, we assume fixed transmission power for both 802.15.4 and 802.11. There are several transmit power control algorithms available for 802.15.4 [70], [71] and 802.11 [72], [73]. However, a recent study [74] demonstrates that the notion of power control can adversely affect the network throughput in presence of multi-hop data transmission over mesh connectivity. Now, in our proposed network architecture, we attempt to simultaneously increase network throughput and decrease energy consumption per transmitted bit through utilizing high-bandwidth radios in a network experiencing multi-hop data transmission. Consequently, considering the adverse impact in the case of such multi-hop data transmission, we do not consider power control in our work.

Besides, in the case of node placement, we assume randomly placed originator nodes in the network. Therefore, we consider evenly distributed accumulator nodes such that each 802.11 can backpack the sensed data from almost the same number of originator nodes. In the expected case, we estimate the number as $\eta = \frac{N_o}{N_a}$, where N_o and N_a are the numbers of originator and accumulator nodes.

Let the average number of hops from an originator node to an accumulator node be $\bar{n}_{15\_4}$. We can estimate

$\bar{n}_{15\_4}$ as $\frac{(2+\sqrt{2})\times\sqrt{\eta}+3}{6}$ assuming minimum-hop routing over randomly placed originator nodes in a square network coverage area where the random placement follows a uniform distribution.

We estimate average transmission energy consumption per second by an originator node as follows:

$$\xi_{tx\_o} = \frac{(N_s + N_{r\_15\_4}) \times \bar{l}_{p\_15\_4}}{BW_{15\_4}} \times P_{tx\_15\_4} \tag{1}$$

where N_s and $N_{r\_15\_4}$ are the average number of transmissions of self-sensed packets and relay packets at an originator node in one second. We estimate $N_{r\_15\_4}$ by taking the average number of packets received from the minimum number of hops (i.e., 1) to the maximum number of hops (i.e., $2 \times \bar{n}_{15\_4} - 1$). Besides, $\bar{l}_{p\_15\_4}$ is the average number of bits in each transmitted packet, BW_{15_4} is the bandwidth, and $P_{tx\_15\_4}$ is the transmission power of 802.15.4.

In our estimation of the average transmission energy consumption per second in Eq. 1, the first multiplicand in the right hand side calculates average time spent in transmission mode by an originator node within one second of its operation and the second multiplicand gives power consumption by the node in transmission mode. Performing similar type of multiplications, we estimate average reception (ξ_{rx_o}) and sleep (ξ_{sl_o}) energy consumption per second by an originator sensor node as follows:

$$\xi_{rx\_o} = \frac{N_{r\_15\_4} \times \bar{l}_{p\_15\_4}}{BW_{15\_4}} \times P_{rx\_15\_4} \tag{2}$$

$$\xi_{sl\_o} = \left(1 - \frac{(N_s + 2 \times N_{r\_15\_4}) \times \bar{l}_{p\_15\_4}}{BW_{15\_4}}\right) \times P_{sl\_15\_4} \tag{3}$$

where $P_{rx\_15\_4}$ and $P_{sl\_15\_4}$ are the reception power and sleep power of 802.15.4. Here, we assume duty cycling for the 802.15.4 radio. We adopt the overhead of duty cycling, caused by idle-mode power consumption, within the sleep power that is utilized in the model. Consequently, to adopt the overhead, we calculate the sleep power as a weighted sum of original idle-mode and sleep-mode powers (see explanation on the weighted sum in Section III-A). Besides, it is worth mentioning that we make the assumption of duty cycling, while deploying high-bandwidth 802.11 in addition to the low-bandwidth 802.15.4, to achieve a delicate trade-off between minimizing power consumption in the network and maximizing network throughput. The objective of minimizing power consumption is to sustain with well-known energy constraint of wireless sensor networks, whereas the objective of maximizing network throughput is to support high-data-rate transmission over the network. Here, the duty cycling, in addition to deploying low-power 802.15.4, ensures minimization of power consumption through enabling the radios to be in sleep mode. The sleep mode power consumption is about $\frac{1}{80}$ times and $\frac{1}{40}$ times compared to idle mode power consumption in the case of 802.15.4 and 802.11 respectively (Table 1). Consequently, the notion of duty cycling can lead to a significant reduction in the power consumption of a wireless sensor network. On the other hand, the deployment of high-bandwidth 802.11 ensures maximization of network throughput through quickly carrying high-rate data utilizing the high bandwidth.

Additionally, it is worth mentioning that we perform our energy modeling based on packet profiling, i.e., based on the number of transmitted and received packets. Therefore, we adopt consistent probability models for duty cycling. More general distribution models for duty cycling will be required in case of considering variations in different timers such as sleep timer, listen timer, etc. As we adopt fixed values for these timers, we do not emphasize on more general distribution models for duty cycling. Nonetheless, such general distribution models can be found in [75]. We need to incorporate these models with our model in case we want to analyze the impact of variations in different timers in our proposed architecture.

Now, combining all the power components, we deduce the average power consumption by an originator node, P_o as

$$P_o = \xi_{tx\_o} + \xi_{rx\_o} + \xi_{sl\_o} \tag{4}$$

Similarly, we can find the average power consumption by an accumulator node, P_a as follows:

$$P_a = \xi_{tx\_a} + \xi_{rx\_a} + \xi_{sl\_a} \tag{5}$$

where ξ_{tx_a}, ξ_{rx_a}, and ξ_{sl_a} are transmission, reception, and sleep energy consumption per second by an accumulator node. Performing similar type of multiplications as done in Eq. 1-3, we deduce each of these components as

$$\xi_{tx\_a} = \frac{N_{r\_B} \times \bar{l}_{p\_B}}{BW_B} \times P_{tx\_B} \tag{6}$$

$$\xi_{rx\_a} = \frac{N_{r\_B\_B} \times \bar{l}_{p\_B}}{BW_B} \times P_{rx\_B} + \frac{N_{r\_B\_15\_4} \times \bar{l}_{p\_15\_4}}{BW_{15\_4}} \times P_{rx\_15\_4} \tag{7}$$

$$\xi_{sl\_a} = \left(1 - \frac{(N_{r\_B} + N_{r\_B\_B}) \times \bar{l}_{p\_B}}{BW_B}\right) \times P_{sl\_B} + \left(1 - \frac{N_{r\_B\_15\_4} \times \bar{l}_{p\_15\_4}}{BW_{15\_4}}\right) \times P_{sl\_15\_4} \tag{8}$$

where $\bar{l}_{p\_B}$ is the average number of bits in each packet transmitted over 802.11 and BW_B is the bandwidth of 802.11. Besides, P_{tx_B}, P_{rx_B}, and P_{sl_B} are the transmission, reception, and sleep power of 802.11 respectively. In addition, N_{r_B} is the number of relay packets transmitted over 802.11, which consists of relay packets received by both 802.15.4 ($N_{r\_B\_15\_4}$) and 802.11 ($N_{r\_B\_B}$). We estimate $N_{r\_B\_15\_4}$ by assuming reception of packets from η nodes at $\bar{n}_{15\_4}$ hops away. We estimate $N_{r\_B\_B}$ similarly. We utilize the ratio between the total network coverage and the transmission coverage of 802.11 to compute the average number of hops from an 802.11 to the base station, $\bar{n}_B$, which we use to calculate $N_{r\_B\_B}$.

Note that in Eq. 6, 7, and 8, we consider fixed bandwidth for 802.11. However, 802.11 can be rate-controlled through adopting different rate adaptation mechanisms [76]–[83]. If we would accommodate any such rate adaptation mechanism, then we need to put corresponding mathematical formulation of the rate achieved over 802.11 [81]–[84] in place of BW_B in the equations.

It is worth mentioning that the sleep energy of 802.11, i.e., the first component in the expression of ξ_{sl_a}, decreases with an increase in the number of the relay packets. In a high-data-rate sensor network, the number of relay packets is indeed very high. Therefore, the sleep energy of 802.11 is confined to a small value, indicating most of its operational period in either transmission or reception mode. Therefore, the high value of sleep power of 802.11 (Table 1) does not exhibit a significant impact in our architecture. Besides, a network typically requires a small number of 802.11 in the case of our proposed energy-efficient architecture. We confirm this requirement of a small number of 802.11 in the next subsection. The small number of 802.11 further decreases the significance of their high sleep power.

Combining all the power components in Eq. (1-8), we estimate the total power consumption over the network as

$$P_{total} = N_o \times P_o + N_a \times P_a \tag{9}$$

Here, the first term in addition in the right hand side calculates the energy consumed by all originator nodes and the second term calculates the energy consumed by all accumulator nodes in the network. In calculation of the first term, we need to combine Eq. (1-4). Similarly, in calculation of the second term, we need to combine Eq. (5-8).

Next, we calculate the network throughput for UDP as

$$T_{total} = N_o \times N_s \times \bar{l}_p \times (\rho_{15\_4})^{\bar{n}_{15\_4}} \times (\rho_B)^{\bar{n}_B} \times \frac{N_a}{N_{a\_cs}} \tag{10}$$

where $\bar{l}_p$ is the average number of bits in the sensed data and N_{a_cs} is the number of accumulator nodes within the carrier sensing region of an 802.11. Here, $\frac{N_a}{N_{a\_cs}}$ indicates the average number of simultaneously transmitting 802.11 over the whole network. Besides, ρ_{15_4} and ρ_B are the probabilities of successful single-hop deliveries over 802.15.4 and 802.11 respectively. We determine the probability of success (ρ) using the probability of failure (ρ'), where we define $\rho' = \rho'_i + \rho'_{ee} + \rho'_{q\_drop}$. Here, ρ'_i, ρ'_{ee}, and ρ'_{q_drop} are the probabilities of transmission failure due to transmission from an interferer, due to environmental effects, and due to drop at the queue of a node respectively. The major component among these values is ρ'_i, which signifies transmission failures at the MAC layer. We separately estimate ρ'_i for the two radios as

$$\rho'_{i\_15\_4} = (\pi \times r^2_{tx\_15\_4}) \times d_{15\_4} \times \left(\frac{\bar{l}_{p\_15\_4}}{BW_{15\_4}}\right)^2 \tag{11}$$

$$\rho'_{i\_B} = (\pi \times r^2_{if\_B} - A_c) \times d_B \times \left(\frac{\bar{l}_{p\_B}}{BW_B}\right)^2 \tag{12}$$

where $r_{tx\_15\_4}$ is the transmission range of 802.15.4, r_{if_B} is the interference range of 802.11, and d denotes the density of the corresponding radio. Besides, A_c is the common area between the carrier sensing region of a transmitting node and the interference region of the receiver node placed at the average distance of one hop away from the transmitting node. Here, we consider only the hidden stations as the interferers in the case of 802.11 due to the use of RTS/CTS. Note that the usage of RTS/CTS can be replaced by a different rate adaptation mechanism pertinent for 802.11 [76]–[83], as RTS/CTS may not be required in case of small-sized sensed packets [85], [86]. In such a case, we need to put corresponding mathematical formulation of the rate achieved over 802.11 [81]–[84] in place of BW_B in Eq. 6, 7, 8, and 12. Nonetheless, in case of variable-sized sensed packets, we need to consider the modified equations up to the threshold above which RTS/CTS is activated and we need to consider our formulated equations afterwards.

In both Eq. 11 and Eq. 12, the first multiplicand in the right hand side calculates the area of interference and the second multiplicand denotes average node density. These two terms combined calculates average number of interferers. Additionally, the third multiplicand in the right hand side calculates probability of two simultaneous data transmission attempts.

In addition to computing ρ'_i, we estimate ρ'_{ee} considering RSS [84], [87] to emulate the *Physical Model*. Besides, we introduce ρ'_{q_drop} by considering the arrival and processing rates at the queue as presented in [84]. Nonetheless, it is worth mentioning that probability of packet drops due to duty cycling will also contribute in determining the probability of failure, i.e., ρ'. However, such probability owing to duty cycling will be very small in case of high-data-rate transmission. As we consider only high-data-rate transmission in this paper, we do not incorporate the probability in the calculation of ρ'.

Finally, we estimate the average energy per bit, ζ, by taking the ratio between P_{total} and T_{total} as follows:

$$\zeta = \frac{P_{total}}{T_{total}} \tag{13}$$

Consequently, our goal of finding the optimal density of 802.11 radio ends up with a minimization problem as

$$d_{B\_opt} = \min_{d_B}(\zeta) \tag{14}$$

It is worth mentioning that we focus on the notion of average energy per bit as the performance metric throughout the whole paper. There are some other performance metrics, such as network lifetime, which are relevant in this regard. However, the lifetime of a network vastly depends on the initial energy availability that significantly differs over various architectures consisting different number of accumulator nodes. On the other hand, the average energy per bit depends only on throughput and power consumption, which are invariant to the initial energy availability. Consequently, we argue that the consideration of average energy per bit in

the network is more relevant than network lifetime in the case of our architecture consisting different types of sensor nodes. Nonetheless, we also discuss the impact of our proposed architecture on network lifetime later in this paper (Section V).

Now, the value of ζ, found from our formulation (Eq. 13), varies depending on the density of the accumulator node, i.e., the density of 802.11. It would be convenient if we could deduce a closed form for the optimal density, i.e., d_{B_opt}. However, the density depends on N_a, which exhibits a number of intricate relationships in the expression of ζ. For example, N_a appears as a denominator in the expression of η, η appears as a square-root in the expression of $\bar{n}_{15\_4}$, and $\bar{n}_{15\_4}$ appears as an exponent in the expression of T_{total}. The presence of several such intricate relationships of N_a inhibits the deduction of a closed form for the optimal density. Therefore, we deduce the optimal density by analyzing the variation in ζ in response to the change in d_B (which also reveals the variation in ζ in response to the change in N_a) through numerical simulation.

C. NUMERICAL OPTIMIZATION OF DENSITY OF THE BACKPACK RADIO

In this section, we analyze the impact of the density of 802.11, i.e., the *Backpack* radio, using our mathematical model to identify its optimal density. We consider an example scenario with a coverage area of 250 $\times$ 250m^2 having 100 originator nodes. Each originator node transmits 50 packets per second destined to the base station, which is located at the corner position of (250m, 250m). Each packet contains 64 bytes application payload.

First, we vary the number of nodes containing 802.11, from 0 to 25 over the whole coverage area, to analyze the impact of such variation in proximity to the optimal density of 802.11. We present the impact of such variation to focus on the phenomena experienced at the low deployment density of 802.11, which is of the utmost significance in our study. Nonetheless, we will also present an extensive numerical analysis of the phenomena, varying the number of nodes containing 802.11 from 0 to 100, later in this section (Fig. 8).

In our numerical analysis, we denote the number of 802.11 in 100 $\times$ 100m^2 area as its density. We can get the exact number of 802.11 from the density value through multiplying it by 6.25 (as $\frac{250\times250m^2}{100\times100m^2} = 6.25$). We present our analysis in terms of density rather than in terms of the exact number of 802.11. We do so to make the analysis more general, as we can utilize the density analysis presented in the paper in similar and proportionate networks, whereas the exact number is applicable only to the networks having exactly same configurations as we consider here. Besides, for the system specifications of the radios in our analysis, we use similar attributes of 802.15.4 and 802.11 as stated in Section III.

We start with analyzing the impact of variation in the density of 802.11 over average energy consumption per transmitted bit in the network. Fig. 7a shows the average energy per bit as the density of 802.11 varies. For clarity, we omit the large value corresponding to using zero 802.11 in the figure, which is consistent with our earlier finding found in Section III-D (see Fig. 5). The figure shows that the average energy per bit decays as the density of 802.11 increases at the beginning, and then starts to increase after reaching an optimal density of the 802.11.

To gain insight into this phenomenon, we measure the variation in the total network throughput and total power consumption in the network. Fig. 7b shows that the total network throughput is very low without any 802.11, which indicates the impotency of the sole deployment of 802.15.4 to carry sensed data to the base station. With the deployment of the first accumulator node, i.e., the first 802.11, the total network throughput decreases due to the high interference around the sole accumulator node. However, deploying further 802.11 increases the total network throughput due to their parallel and distributed data collection over the network, and their usage of high bandwidth in the distributed data collection. However, the rate of the throughput increase decays with the increase in the density. Later, we will show that such a trend over the increase in throughput indeed exists in real cases using testbed results in Section V.

On the other hand, Fig. 7c shows that the total power consumption in the network with no 802.11 is higher than that with 802.11 at a few initial points. This happens due to the large number of hops traversed over 802.15.4 to eventually reach the base station in the absence of any 802.11. After deploying the first 802.11, the total power consumption starts to increase as the density of 802.11 increases. The rate of the increase is small at a few initial points, and then starts to intensify with significant margins with subsequent increases in the density. This trend in total power consumption results from a combined effect of power consumption by an originator node and by an accumulator node following Eq. 9.

The power consumption of an originator node decreases with an increase in the density of 802.11, which we depict in Fig. 7d. The reason behind this trend is the offloading of part of the transmission and reception tasks from the originator node through the deployment of the 802.11. Here, the rate of decrease gradually diminishes following the law of diminishing returns [88].

Additionally, in the case of an accumulator node, power consumption increases at some initial points with an increase in the density of 802.11, and then starts to gradually decrease. Fig. 7e depicts this trend. Here, the increasing points have three different trends over the rate of the increase. At a few initial points, the rate is very low. This happens due to the high extent of collision over the transmission of sensed data, sent by originator nodes, in the presence of a few target accumulator nodes with 802.11. Therefore, the accumulator nodes do not have a large volume of data to relay to the base station and thus exhibit low power consumption. After these initial points, the extent of collision gets reduced due to the increased number of accumulator nodes. This increase in turn boosts transmission and sensing tasks of the accumulator nodes. Consequently, the rate of increase in their

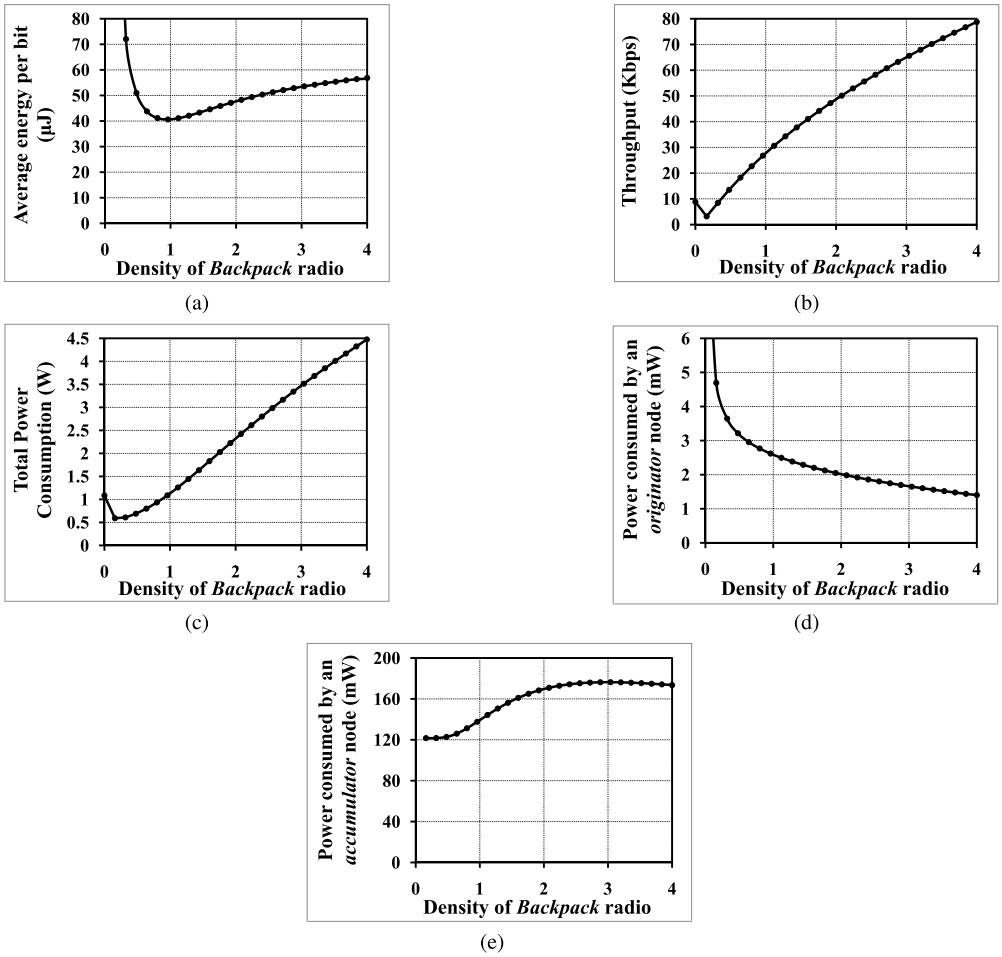

FIGURE 7. Impact of variation in density of the *Backpack* radio in proximity to its optimal density. (a) Average energy per bit. (b) Network throughput. (c) Total power consumption. (d) Power consumption by an originator node. (e) Power consumption by an accumulator node.

power consumption also increases. After these points with higher rates of increase, the transmission and sensing tasks of an accumulator node again start to gradually diminish. This happens due to a decrease in the average number of originator nodes per accumulator node. The diminishing trend in the rate of increase in power consumption by accumulator nodes eventually leads to a negative value for the rate of increase after a certain point (density = 3.04). Therefore, the power consumption by accumulator nodes starts to decrease onward. The combined effect of the power consumption of an originator and of an accumulator node along with the varying number of the accumulator nodes determines the total power consumption in the network. Here, it is worth mentioning that the accumulator nodes consume higher power than the originator nodes due to the presence of 802.11.

The overall impact of total power consumption and total network throughput results in such a trend in average energy per bit that we can find the existence of an optimal density of 802.11 (0.96 in Fig. 7a). We have to confine the density of 802.11 close to the optimal point to achieve the best trade off between the total network throughput and the total power consumption in the network.

Up to this point, we analyze energy efficiency of Backpacking close to the point of the optimal density of 802.11. Now, we attempt to provide an extensive analysis in this regard. In the extensive analysis, we analyze the energy efficiency for all possible densities of 802.11. To do so, we consider the density from 0 to 16 to mimic the number of accumulator nodes from 0 to 100, i.e., up to the total number of originator nodes. Fig. 8 depicts various components that are required to analyze the energy efficiency corresponding to such variation.

In the extensive analysis, we reveal a new trend in total network throughput that was not present in the case of the analysis in proximity to the optimal density of 802.11. Fig. 8b depicts the complete trend in total network throughput. Here, the throughput increases up to a certain density of 802.11, and then starts to decrease with a decreasing rate onward. The initial increase is achieved by exploiting the high bandwidth of 802.11. On the other hand, the subsequent decrease in throughput occurs due to the long transmission range of 802.11. The long transmission range eventually results in

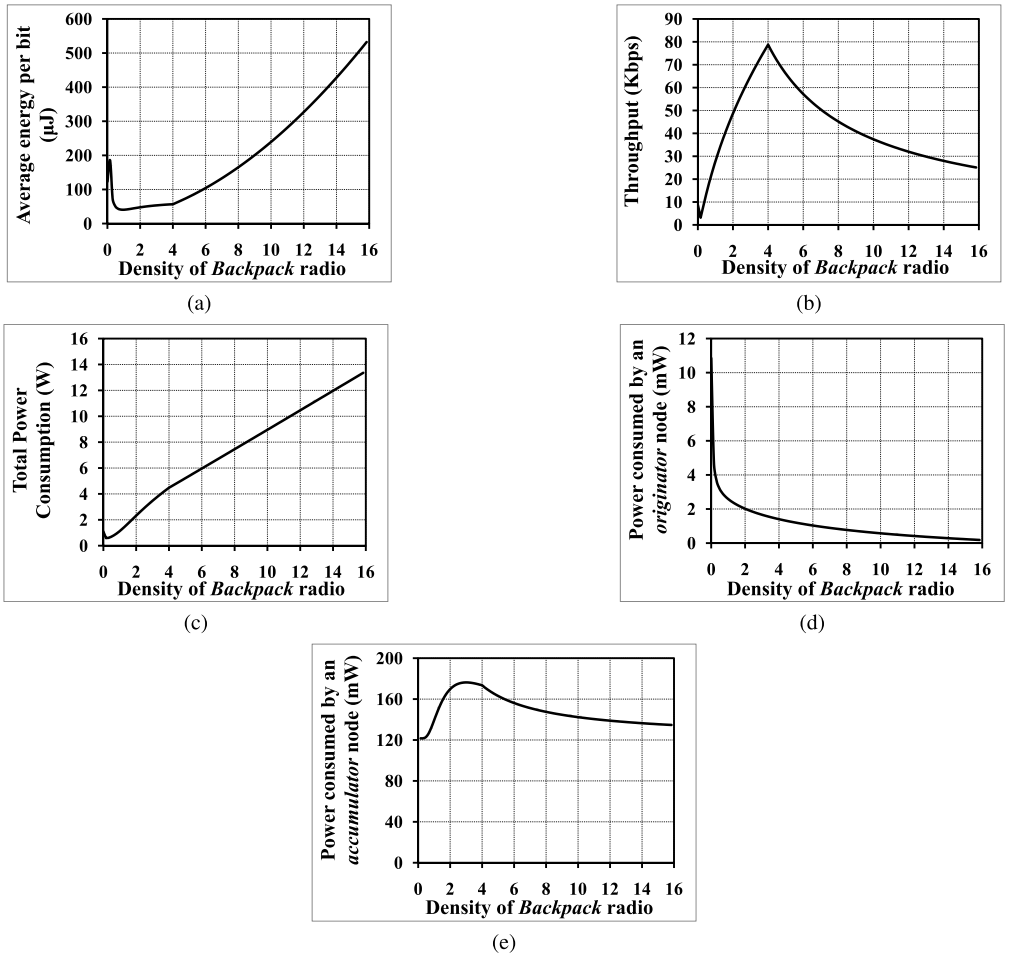

FIGURE 8. Impact of all possible variation in the density of *Backpack* radio. (a) Average energy per bit. (b) Network throughput. (c) Total power consumption. (d) Power consumption of an originator node. (e) Power consumption of an accumulator node.

large footprints, which in turn result in a high extent of interference even in the presence of RTS/CTS. We have already discussed the tradeoff between these two opposing phenomena in Section III-D.

We achieve the highest total network throughput at the density of 4 (or equivalently 25 802.11s in the network) in our numerical simulation. Thus, the density of 4 is the optimal one in terms of total network throughput. Therefore, we can also utilize our model to determine the density required for the highest throughput.

In our extensive analysis, we can find two different trends in the power consumption of an originator node and of an accumulator node. Fig. 8d and Fig. 8e depict these two trends respectively. Here, these trends are similar to the trends that are already described in the analysis in proximity to the optimal density of 802.11. The combined effect of these two trends results in a near-linear increasing phenomena in total power consumption in the network, with an increase in the density of 802.11.

In addition to the trend in total power consumption, we also present a breakdown of the power consumption of 802.15.4 and of 802.11 in the network. Here, we present the breakdown in three cases: with no 802.11, with an optimal number of 802.11, and with 802.11 in all sensor nodes. Fig. 9 depicts the breakdown. This figure reveals that power consumption of 802.15.4 is significantly reduced at the optimal density of 802.11 so that the high power consumption of 802.11 can be compensated by the reduction.

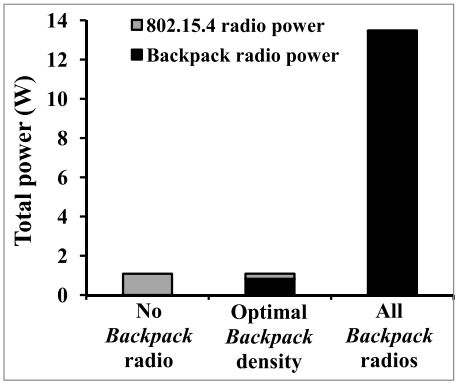

FIGURE 9. Breakdown of total power consumption in the network.

Note that the individual power consumption of 802.11 is significantly higher than that of 802.15.4 even at the optimal number of 802.11 as shown in Fig. 9. Therefore, the initial energy of accumulator nodes containing 802.11 needs to be high compared to that of originator nodes containing only 802.15.4. However, the number of such high-power nodes in the network is small at the optimal deployment density. Consequently, we need to supply high amount of energy to only a small number of nodes in our proposed architecture. Note that even in case of failure of the high-power nodes due to energy depletion or any other reasons such as hardware failure, the whole network turns back to a classical wireless sensor network consisting only 802.15.4, and thus continue its operation over only 802.15.4. If the network is unable to continue its operation in the classical topology and demands existences of the accumulator nodes (see *Case 1* in Section VII), then we need to analyze the impact of failure of accumulator nodes in a more sophisticated manner through analyzing the network-level reliability of our proposed network architecture. Such an analysis [89] is beyond the scope of this paper.

Now, the trends in total power consumption and in total network throughput simultaneously control average energy consumption per transmitted bit in the network. Up to the optimal density for total network throughput, the trend in average energy per bit follows the analysis, which we have already presented. After this point, average energy per bit starts to increase with an increasing rate as the total network throughput starts to decrease from this point. Here, we can find the highest average energy per bit in the case of the highest density of 802.11. This scenario is somewhat similar to the complete replacement of 802.15.4 by 802.11. Therefore, this result again reveals that a complete replacement of 802.15.4 by a high-bandwidth radio, 802.11 in our case, will *not* be an energy-efficient solution. We have also revealed the similar finding in Section III-D.

It is worth mentioning that we consider random placements of originator nodes containing only 802.15.4 and uniform placements of accumulator nodes containing both 802.11 and 802.15.4 in our analysis presented in this paper. In case of non-uniform placements of accumulator nodes, their deployment should be carefully planned for optimizing the performance of the network. For example, in case of clustered originator node deployment around several hotspots, the deployment of accumulator node should also follow the hotspots distribution. Determining such deployment of accumulator node for optimizing network performance is known to be NP-hard [90], [91] and several heuristic-based mechanisms [90]–[93] are available in the literature for similar node deployment problems. Nonetheless, optimizing deployment of the originator nodes is also a complex problem, which depends on multiple parameters [94] such as routing, power management, location management, etc. Few research studies in the literature have investigated similar node deployment problems [95]. In case of such optimization in the deployment of originator nodes, we also need to carefully plan deployment of accumulator nodes after performing the optimization in our proposed architecture.

Up to this point, we present numerical outcomes from our formulated mathematical model. Next, we validate the outcome of our model through experiments over a real testbed. The outcomes of the experiments also evaluate the efficacy of our proposed network architecture. We present the validation and the evaluation in the next section.

V. TESTBED EVALUATION

In this section, we evaluate the efficacy of the proposed hybrid architecture on a wireless sensor network testbed. In our evaluation, we also validate the optimal density of 802.11 derived in the previous section. Before presenting the evaluation results, we briefly describe the testbed settings.

A. TESTBED SETTINGS

We arrange a testbed consisting of twenty randomly placed originator nodes.[2] We use TelosB motes [2] as the originator nodes each equipped with a 250Kbps 802.15.4 radio in our testbed experiment. We program the TelosB motes to a low transmission power level using TinyOS 2.x [97] to impose multi-hop transmission during the experiment. Each originator node transmits 25 UDP packets per second, each consisting of 28 bytes of application payload. These nodes continue transmission for 30 seconds after an initial delay of 105 seconds. We utilize the initial delay to let the originator nodes develop stable routing path information.

In our experiment, we utilize a Beagleboard [98] to build a dual-radio accumulator node. A Beagleboard consists of a $3.1'' \times 3''$ PCB. The board contains a 1 GHz Cortex A8 DM3730CBP processor [99]. The processor has 800 MHz DSP speed and 200 MHz SGX speed. The board also contains a 200 MHz MDDR SDRAM having a capacity of 512 MB as its memory. The processor and memory are connected using a technique called Package on Package (POP) that exhibits a compact way to mount the memory on top of the processor to reduce the size of the unit. The small size, along with high-speed processor and memory having a considerably low power consumption, presents the suitability of a Beagleboard as a pragmatic choice for the dual-radio accumulator node in wireless sensor networks.

Now, the Beagleboard does not have any radio connected to it. Therefore, we externally connect a TelosB mote and a Trendnet Dongle [100] to it through USB ports. Here, we utilize the 802.15.4 radio of the TelosB mote and the 802.11 radio of the Dongle in our experiment. During the experiment, we set the channels of 802.15.4 and 802.11 radios to two non-interfering channels. A Beagleboard along with these two external radios serves as an accumulator node in the testbed. We provide a snapshot of this accumulator node in Fig. 10. This figure shows both a board view (Fig. 10a) and a cached view (Fig. 10b) of an accumulator node.

[2]Similar small-scale testbeds already exist [96] for performance evaluation of wireless sensor networks.

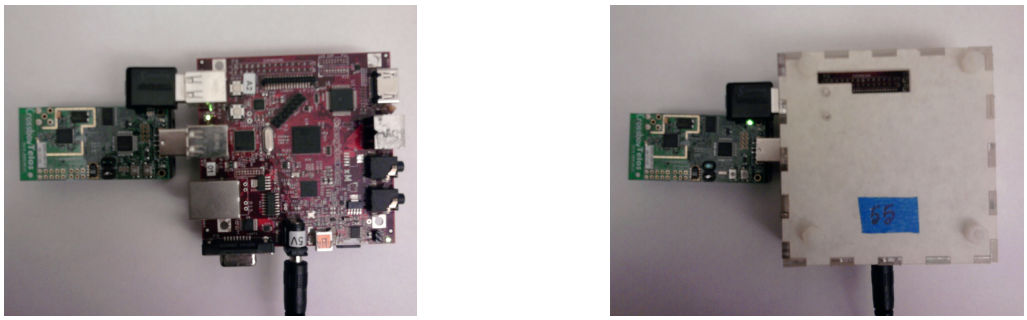

(a) (b)

FIGURE 10. A custom-assembled accumulator node used in testbed evaluation. (a) Board view. (b) Cached view.

In our testbed, we randomly place the originator nodes. However, we uniformly place the accumulator nodes so that they backpack the sensed data of about the same number of originator nodes. We utilize the power ratings presented in Table 1 along with the radio startup power to calculate the energy consumption of all the nodes in the testbed. Here, it is worth mentioning that the consideration of duty cycles in the ratings (Section III-A) emulates the LPL [101] of TinyOS.

We adopt a dynamic, table-driven routing mechanism for transmission over both 802.15.4 and 802.11 in our experiment. The mechanism resembles the loop-free, minimum-hop routing considered in Section IV-A. In our testbed, each node periodically transmits routing control packets at an interval of 5s indicating its minimum-hop distance to the base station. These periodic control messages help to update the entries of the routing table in each sensor node.

We consider the number of hops to the base station[3] as the primary routing metric and the number of successors as the secondary routing metric to update the entries in the routing table. The entries in a routing table maintain soft states, i.e., each table entry expires after a certain interval (20s in our experiment). The soft states ensure freshness of the routing table entries. However, due to the maintenance of the soft states, a node may not have any routing information for a period of time due to the intermediate drops of control packets. In such situations, we impose broadcasting of sensed data.

We utilize our mathematical model to compute the optimal number of 802.11 in our testbed setting. The model indicates the optimal number as 2 following Eq. 14. Therefore, we perform our experiment in five different settings: with no 802.11 and with 1 $\sim$ 4 802.11s. We present a snapshot of the testbed setting having 2 802.11s in Fig. 11.

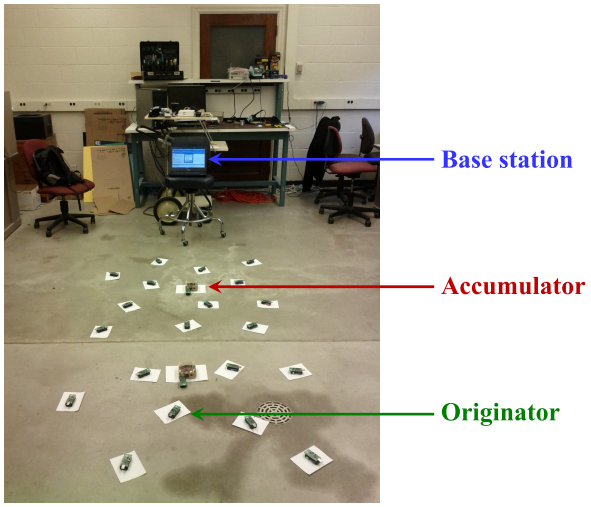

FIGURE 11. Testbed setting.

B. EXPERIMENTAL RESULTS

We start our experimental evaluation by focusing on two metrics: total network throughput and total power consumption. The comparisons over these two metrics eventually lead to the evaluation of average energy consumption per transmitted bit. We count the total number of transmitted and received bits at each sensor node and then calculate its total power consumption considering the bandwidth of its radio along with the power measurements in different operational modes of the radio. Besides, we consider duty cycling for 802.11 in our calculation. The 802.11s in our testbed only directly transmit data, which is accumulated by the 802.15.4 of corresponding accumulator nodes, towards the base station. Here, the base station always remains active for data reception. Therefore, the duty cycling of 802.11s of the accumulator nodes[4] will only influence their power consumptions, exhibiting no influence on network throughput. Consequently, the consideration of duty cycling in the calculation of the power consumption of 802.11s does not result any deviation from reality in the calculation of network throughput.

Exploitation of 802.11 boosts the total network throughput (Fig. 12a) over the testbed. This increase results from the high number of packets received at the base station. Fig. 13 depicts the phenomena of receiving a high number of packets

[3]The actual values of the number of hops vary from 1 to 5 over different settings. Besides, average values of the number of hops remain within the range of [2, 3] in all settings.

[4]We can use batteries to power accumulator nodes having 802.11, as recent designs of sensor modules incorporating 802.11 promises to do so [102].

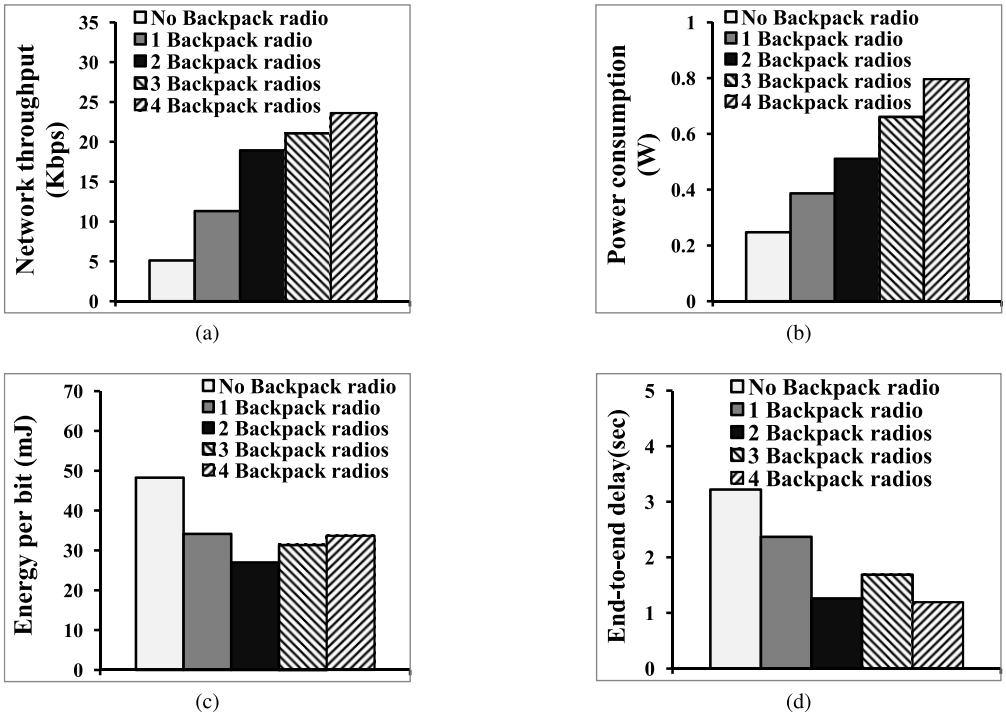

FIGURE 12. Network performance in five different testbed settings. (a) Total network throughput. (b) Total power consumption. (c) Average energy per bit. (d) End-to-end delay.

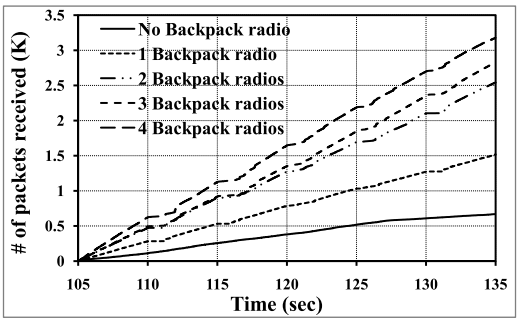

FIGURE 13. Number of received packets at the base station.

with 802.11. This figure also shows that the number gradually intensifies with an increase in the number of deployed 802.11. However, the rate of the intensification gradually decreases with the increase in the number of 802.11 following the law of diminishing return [88]. This trend eventually results in a similar phenomena, i.e., the diminishing return, in the case of total network throughput. Fig. 14a shows the phenomena over the increase in total network throughput.

We achieve the increased total network throughput at the expense of an increase in total power consumption over the network (Fig. 12b). Here, we reveal a near-linear trend in the increase in total power consumption. Fig. 14b depicts the near-linear trend. The combined effect of this near-liner increase and the diminishing increase in the case of network throughput results in a similar trend in energy per bit that we have already discussed in Section IV-C while focusing on Fig. 7a. Fig. 12c depicts the trend in energy consumption per transmitted bit with a variation in the number of accumulator nodes. The trend in this figure resembles the trend in Fig. 7a. Here, we achieve 29%, 44%, 35%, and 30% decreases in energy per bit with 1, 2, 3, and 4 accumulator nodes, having 802.11, respectively compared to no accumulator node. The extent of these improvements reveal that 2 is indeed the optimal number of accumulator nodes for energy efficiency in terms of energy per bit. Therefore, the testbed results validate the outcome of our proposed mathematical model.

Besides, we achieve decreased end-to-end delay with 802.11 due to the low end-to-end delay property of the low density 802.11. Fig. 12d shows end-to-end delays for different settings with 802.11. Here, we observe 26%, 61%, 47%, and 67% decreases in the end-to-end delay with 1, 2, 3, and 4 802.11s respectively in comparison to no 802.11.

Next, we analyze energy consumption of the originator nodes deployed over the testbed in Fig. 15. Here, we utilize line graphs to present high-level views of relative total energy consumption and relative standard deviation in energy consumption in different settings. Here, relatively higher placement of a graph pertinent for a setting (for example with no Backpack radio in Fig. 15a) indicates relatively high energy consumption in that case. Besides, relatively higher fluctuation over a graph pertinent for a setting (for example with no Backpack radio in Fig. 15a) indicates relatively high standard deviation in that case.

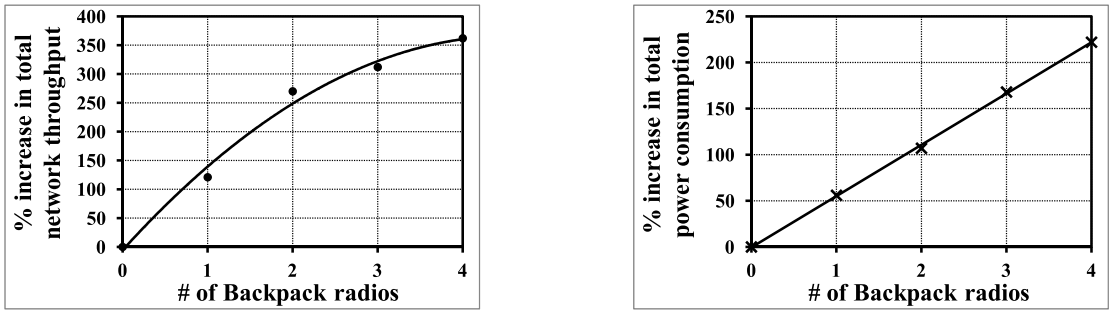

FIGURE 14. Different trends over percentage increases in total network throughput and total power consumption with a variation in the number of *Backpack* radios. (a) Percentage increases in total network throughput. (b) Percentage increases in total power consumption over the network.

In Fig. 15, we first present total energy consumption of these nodes in Fig. 15a. Here, we find that the decreased values of total energy consumption for most of the originator nodes are in the settings having 802.11 radios. We analyze the decrease in total energy consumption by focusing on the three components of the energy consumption. Fig. 15b, Fig. 15c, and Fig. 15d show these components, i.e., transmission energy, reception energy, and sleep energy, respectively.

We find that most of the nodes consume decreased transmission and reception energies while deploying 802.11. Nonetheless, such deployments consume increased sleep energy for most of the nodes. Here, it is worth mentioning that the sleep energy is significantly lower compared to both transmission and reception energy, which we have already discussed in Section III-A (using the data presented in Table 1). As a result, even though the sleep energy is increased, total energy consumption of the originator nodes achieves significantly reduced values for most of the nodes in the case of deploying 802.11s.

Besides, Fig. 15a reveals that the total energy consumption with 802.11 exhibits a moderate fluctuation over the reduced values. Therefore, we find decreased standard deviation of the energy consumption in the settings with 802.11. We show the variations in the average and in standard deviation of energy consumption in Fig. 16. We also summarize the extents of the average and standard deviation in Table 2. Here, we observe 24%, 46%, 41%, and 43% decreases in average total energy consumption with 1, 2, 3, and 4 802.11s respectively in comparison to no 802.11. These values are 17%, 50%, 33%, and 33% accordingly in the case of decrease in standard deviation of the total energy consumption of these nodes.

TABLE 2. Average and standard deviation of total energy consumption of all sensor nodes with only 802.15.4 in the testbed evaluation.

Setting	Average (J)	Standard deviation (J)
No *Backpack* radio	0.37	0.12
1 *Backpack* radio	0.28	0.10
2 *Backpack* radios	0.20	0.06
3 *Backpack* radios	0.22	0.08
4 *Backpack* radios	0.21	0.08

Finally, we analyze the ultimate advantage of the decreased average and standard deviation of total energy consumption. Here, we focus on two metrics, First Node Dies (FND) and Half of the Nodes Die (HND), in the analysis. FND indicates the time elapsed before the death of the first node and HND indicates the time elapsed before the death of half of the nodes in the network [103]. We consider both the metrics for the originator nodes containing only 802.15.4. We do not cover the accumulator nodes containing both 802.11 and 802.15.4 in this analysis, as we have assumed that these nodes are deployed with high initial energy (Section IV-C). Due to the higher initial energy of accumulator nodes, computing FND and HND covering accumulator nodes would lead to an unfair treatment to originator nodes.

We present the improvement in FND and HND with different number of Backpack radios in Fig. 17. We also summarize the extents of improvement in Table 3. The results suggest that we can achieve 28%, 58%, 45%, and 68% increases in FND and 35%, 104%, 86%, and 121% increases in HND using 1, 2, 3, and 4 802.11s respectively in comparison to no 802.11. We achieve such improvement due to the low and evenly distributed total energy consumption of the originator nodes.

TABLE 3. Percentages of improvement in first node dies (FND) and half of the nodes die (HND) in comparison to no *Backpack* radio in the testbed evaluation.

Setting	Improvement in FND	Improvement in HND
1 *Backpack* radio	28%	35%
2 *Backpack* radios	58%	104%
3 *Backpack* radios	45%	86%
4 *Backpack* radios	68%	121%

Note that the improvement in FND exhibits higher values in Table 3 compared to that presented in [12] (for the settings with one and two 802.11s to be more specific). This happens as we used larger-size laptops in the experiments presented in [12], whereas we use smaller-size Beagleboards in the experiments presented in this paper as accumulator nodes. The larger size of a laptop along with its top-cover display put obstacles to the 802.15.4 of the attached TelosB

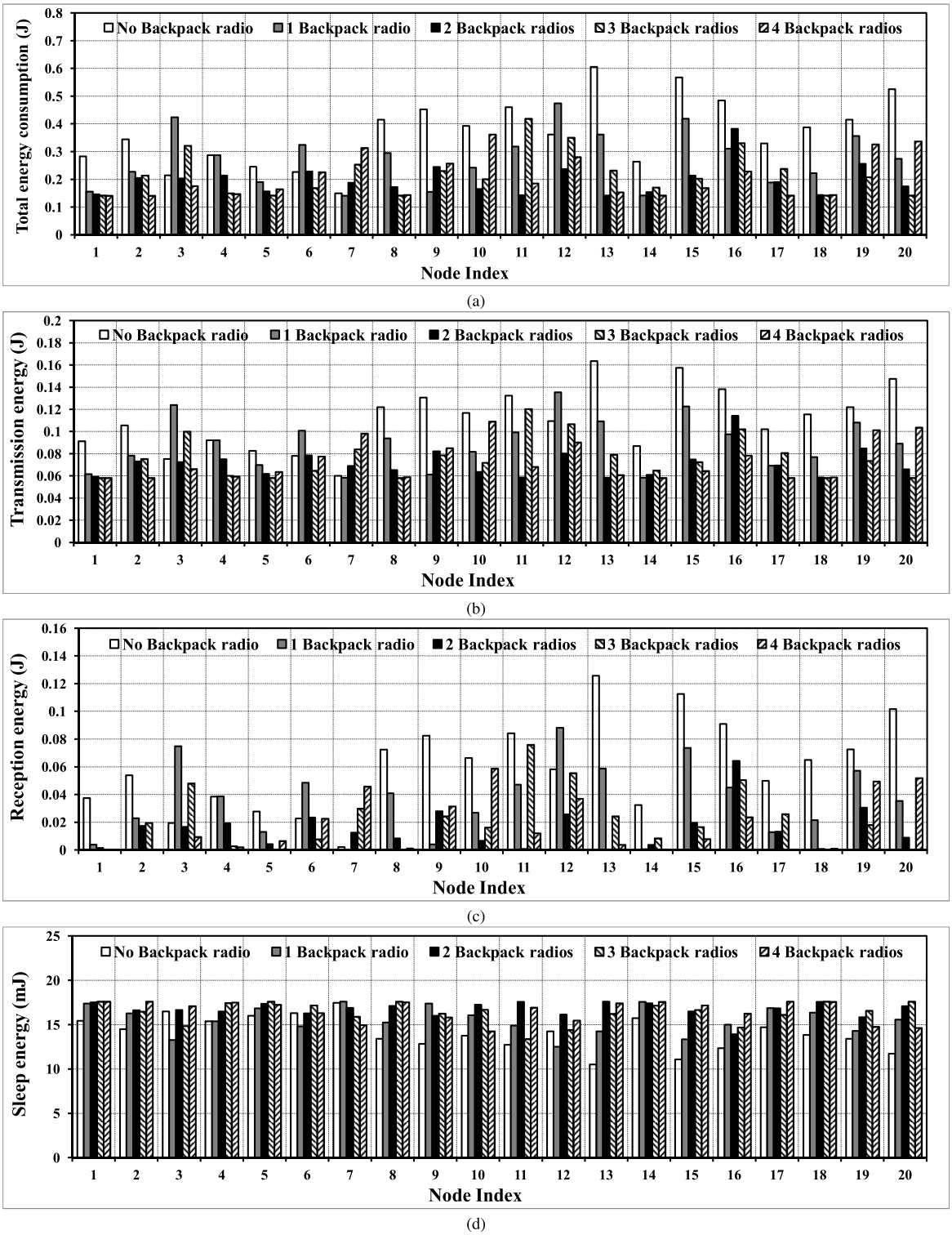

FIGURE 15. Energy consumption by each originator node along with its three components in the testbed evaluation. (a) Total energy consumption. (b) Transmission energy consumption. (c) Reception energy consumption. (d) Sleep energy consumption.

in corresponding accumulator node. The obstacles came into play as we program the TelosB motes to a low transmission power level to impose multi-hop transmission during the experiment, which reduces transmission range of 802.15.4 limiting its ability to successfully transmit data in presence of obstacles. The impact of obstacles became highly significant in case of the setting with one 802.11 or with one accumulator node, as several originator nodes may have to directly

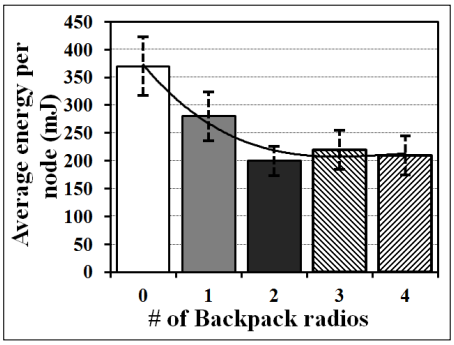

FIGURE 16. Average and standard deviation of energy consumption by originator nodes in the testbed evaluation.

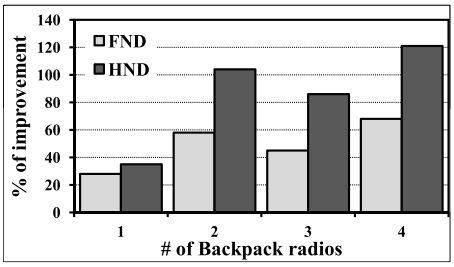

FIGURE 17. Percentages of improvement in FND and HND using different number of Backpack radios compared to using no Backpack radio in the testbed evaluation.

communicate with the base station for not being able to connect to the only-available accumulator node due to the obstacle. Consequently, we ended up with significantly smaller values of FND with 802.11 in [12] compared to that we get in this paper. To validate this argument, we can analyze another direct consequence of the phenomena. The consequence is getting significantly decreased network throughput with one 802.11 in [12]. We can validate this consequence through comparing Fig. 12a with corresponding figure in [12].

Now, we summarize our experimental results. All the experimental results suggest that Backpacking has the potential to enhance energy efficiency of high-data-rate applications. Here, the potential is twofold:

1) It enhances the energy efficiency in terms of a decrease in the energy consumption per transmitted bit over high-data-rate sensor networks. It attains the lower value of energy per bit by achieving significant boosts in network throughput while increasing total power consumption in the network in a relatively lower extent.
2) It increases both the First Node Dies and the Half of the Nodes Die in high-data-rate sensor networks. It achieves the extended durations by offloading originator nodes from a part of their sensing and receiving tasks by suitable exploitation of accumulator nodes.

VI. DISCUSSION

In this paper, we mainly focus on the characteristics of a 802.15.4 radio of a TelosB mote. We achieve the improvement in performance by addressing the short transmission range and low data rate of the low-sleep-power radio. However, there are some other motes, such as IRIS [104] and Micaz [105] with 802.15.4 having higher transmission ranges and higher sleep power than that of a TelosB mote. Besides, other similar alternatives are also available in this regard. Examples include ultra-wide-band (UWB) [106]–[108], which exhibit similar transmission range and power consumption with higher bandwidth [106] compared to that of conventional 802.15.4. If we consider either of these alternatives, we have to plug its characteristics into our mathematical model to compute the optimal density of *Backpack* radios. Here, a more energy-efficient alternative of the considered 802.15.4 is expected to result in a reduction in the *Backpack* density, whereas a less energy-efficient alternative should increase the *Backpack* density in our proposed network architecture.

In addition, we focus on the 802.11b of Stargate as the *Backpack* radio in this paper due to wide acceptability of Stargate in recent applications [20]. Nonetheless, there are also other alternatives for the *Backpack* radio than 802.11b. Examples include 802.11g, 802.11n, and Bluetooth 3.0. Opposing the case with the alternatives of 802.15.4, a more energy-efficient alternative of the considered *Backpack* radio is expected to result in an increase in the *Backpack* density, whereas a less energy-efficient alternative should decrease the *Backpack* density in our proposed network architecture. On the other hand, similar to the case with the alternatives of 802.15.4, we have to plug the associated characteristics of these alternatives of the *Backpack* radio into our model. The outcome of the model leads to achieving energy efficiency over high-data-rate sensor networks utilizing the desired alternative.

There are a number of pragmatic instances of high-data-rate sensor networks, where the notion of Backpacking can be exploited. We have already pointed out several of these instances in Section II-A. It is worth mentioning that we have pointed out two processes for high-rate data generation in that section as: 1) Accumulation of data from low-data-rate applications in a large network, and 2) From high data rate applications itself. We can utilize our proposed architecture irrespective the variation in the process of high-rate data generation in a sensor network. Here, the actual network architecture will vary based on the process of high-rate data generation. This happens as the corresponding network parameters, that eventually determine the optimal number of accumulator nodes, will be different for the networks having two different types of high-rate data generation processes. Further, to provide a complete picture over the applications of Backpacking, we present a comprehensive study on the applications in the next section.

VII. APPLICATIONS OF BACKPACKING: AN EXTENDED VIEW

We have already mentioned in Section II-A that state-of-the-art network architecture can not support high-data-rate transmission in wireless sensor networks, which is our main

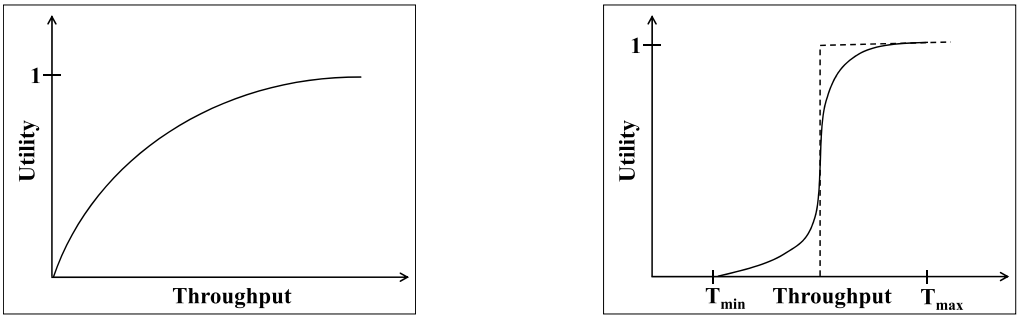

FIGURE 18. Trends in utility functions of elastic and inelastic applications in response to variation in throughput. (a) Utility function of an elastic application. (b) Utility function of an inelastic application.

focus in this paper. Now, analyzing the experimental results in Section V, we have found that Backpacking has the potential to improve energy efficiency from two different perspectives: reducing energy consumption per transmitted bit, and increasing FND and HND. We can utilize these two perspectives for supporting a number of high-data-rate applications over wireless sensor networks. Moreover, such utilization can even cover some applications, which are currently being supported through state-of-the-art network architecture. In the case of such applications, Backpacking enhances network performance exceeding that provided by the state-of-the-art network architecture. Now, to comprehensively analyze all the applicabilities of Backpacking, while covering our main focus on the applications exceeding capability of the state-of-the-art network architecture, we first illustrate a notion called *elasticity* of an application.

Elasticity [109] of an application implies its service level, in terms of its utility or *goodness*, in response to changing values of throughput. We can categorize most of the sensor network applications into two types based on their elasticities: elastic and inelastic applications.

An elastic application presents a non-zero utility as long as it experiences a non-zero throughput following a logarithmic function as follows:

$$U_e(T_e) = \log(T_e + 1)$$

where U_e is utility of the elastic application and T_e is corresponding throughput. Fig. 18a depicts the shape of the utility function of an elastic application. On the other hand, an inelastic application presents a non-zero utility only after it experiences a minimum threshold throughput (T_{min}). Besides, its utility saturates after a maximum threshold throughput (T_{max}). The utility exhibits an "S-shaped" growth [110] in between these two thresholds following a sigmoid function [111] as follows:

$$U_i(T_i) = \begin{cases} 0 & \text{if } T_i < T_{min} \\ \frac{1}{1+e^{-a\times(T_i-b)}} & \text{if } T_{min} \le T_i \le T_{max} \\ 1 & \text{if } T_i > T_{max} \end{cases}$$

where U_i is utility of the inelastic application, T_i is the corresponding throughput, b is the average of T_{min} and T_{max}, and a is a parametric multiplier that controls the slope of the sigmoid utility function. Fig. 18b depicts the shape of the utility function of an inelastic application.

We can find different examples of elastic and inelastic high-data-rate sensor network applications. Structural health monitoring is a prominent example of an elastic high-data-rate sensor network application [112]. On the other hand, aircraft testing is a possible example of an inelastic high-data-rate sensor network application.

In addition to the elastic and inelastic applications, there are also some other high-data-rate applications that impose a minimum requirement on throughput for a non-zero utility and present a logarithmic utility for subsequent increases in the throughput as well. These applications inherit partial characteristics from both elastic and inelastic applications. These applications are frequently referred to as quasi-elastic applications [113]. Seismoacoustic volcanic monitoring is a probable quasi-elastic high-data-rate sensor network application.

Now, addressing the variation in elasticity, we analyze energy efficiency of Backpacking over different types of high-data-rate applications as follows:

- All applications: Backpacking improves two metrics, First Node Dies and Half of the Nodes Die, over high-data-rate sensor networks irrespective of the elasticities of the corresponding applications. This improvement is achieved through the deployment of accumulator nodes, which off-loads the originator nodes resulting in maximization of their lifetimes.
- Elastic applications: Backpacking achieves low energy consumption per transmitted bit for an elastic application through boosting its throughput. The boost in throughput in turn enhances the utility of the elastic application. Therefore, the impact of Backpacking in the case of an elastic application covers two different perspectives: 1) Energy efficiency through utility enhancement of the application traffic and 2) Improvement of FND and HND through the enhancement of lifetimes of most of the sensor nodes in the network.
- Inelastic applications: Energy efficiency of Backpacking, through the enhancement of throughput, vastly depends on the two thresholds: T_{min} and T_{max} in the

case of an inelastic application. Here, we can analyze the energy efficiency in four different cases based on these two thresholds and corresponding network throughput pertinent for two different settings: with no Backpacking (T_{no_B}) and with Backpacking (T_B).

1) *Case 1 ($T_{no\_B} \leq T_{min} < T_B \leq T_{max}$):* If T_{no_B} lies prior to T_{min} and T_B lies beyond T_{min}, then Backpacking is mandatory to be deployed to achieve a non-zero utility from the inelastic application. In this case, Backpacking achieves energy efficiency through boosting the throughput, which in turn improves energy consumption per transmitted bit.
2) *Case 2 ($T_{min} \leq T_{no\_B} < T_B \leq T_{max}$):* If both of T_{no_B} and T_B lie in between T_{min} and T_{max}, then Backpacking again achieves energy efficiency through boosting the throughput. This phenomena in turn improves energy consumption per transmitted bit. Here, Backpacking achieves utility enhancement in a way, which is somewhat similar to the case of an elastic application.
3) *Case 3 ($T_{min} \leq T_{no\_B} < T_{max} \leq T_B$):* If T_{no_B} lies in between T_{min} and T_{max}, and T_B lies beyond T_{max}, then we have to redefine the energy efficiency of Backpacking. In our formulation presented in Section IV-B, we have defined the energy efficiency in terms of energy consumption per transmitted bit, ζ as $\frac{P_{total}}{T_{total}}$, where P_{total} is the total power consumption in the network and T_{total} is the total network throughput. Now, in our current case, we redefine ζ as $\frac{P_{total}}{T_{max}}$. After considering the redefinition, we have to determine the energy consumption per transmitted bit to assess the energy efficiency of Backpacking.
4) *Case 4 ($T_{min} < T_{max} \leq T_{no\_B} < T_B$):* If both T_{no_B} and T_B lie above T_{max}, then the increase in throughput through Backpacking does not result in any utility enhancement. Therefore, this is the only case where the decrease in energy consumption per bit using Backpacking does not have any pragmatic impact.

- Quasi-elastic applications: Finally, we can analyze the energy efficiency of Backpacking for a quasi-elastic application in a way that is similar to the analysis for an inelastic application. A quasi-elastic application does not involve the notion of T_{max} and thus only considers the presence of T_{min}. Therefore, we will have only two cases, which are similar to the first two cases (*Case 1* and *Case 2*) pertinent to the inelastic application.

In summary, Backpacking always improves First Node Dies and Half of the Nodes Die. Besides, it always enhances energy efficiency of an elastic application and a quasi-elastic application through decreasing energy consumption per transmitted bit. Further, it also enhances energy efficiencies of most of the inelastic applications in a similar way.

VIII. CONCLUSION

The demand for high-data-rate transmission has become apparent in the emerging advanced sensor network applications. This paper aims to address the demand by supplementing sensor networks having de facto 802.15.4 with high-bandwidth and transmission-efficient 802.11 to backpack accumulated sensed data towards the base station. Consequently, this paper proposes a novel multi-radio sensor network architecture and addresses the key design challenges of determining optimal deployment density of the transmission-efficient radio in our proposed architecture.

In this paper, a cross-layer mathematical model has been formulated to calculate the optimal density of the transmission-efficient radio in the proposed network architecture. The model characterizes a delicate balance between spatial reuse of short-range transmissions over 802.15.4 and energy-efficiency of long-range, high-data-rate transmissions over 802.11.

A testbed experiment has been conducted to show the effectiveness of the proposed energy-efficient architecture along with accuracy of the mathematical model. The experimental results reveal up to 44% and 67% improvement in average energy per bit and end-to-end delay with the proposed architecture in comparison to that with no transmission-efficient radio. Moreover, the proposed architecture attempts to evenly distribute energy consumption throughout the network. This phenomena eventually results in up to 68% and 121% increases in the time elapsed before the death of the first node and half of the nodes having only 802.15.4 in comparison to the architecture with no transmission-efficient radio. These results confirm that the strategic deployment of transmission-efficient radios can support high-data-rate sensor network applications while achieving high energy efficiency.

REFERENCES

[1] P. Dutta, D. Culler, and S. Shenker, "Procrastination might lead to a longer and more useful life," in *Proc. HotNets*, 2007, pp. 1–7.
[2] J. Polastre, R. Szewczyk, and D. Culler, "Telos: Enabling ultra-low power wireless research," in *Proc. IPSN*, Apr. 2005, pp. 364–369.
[3] R. Cardell-Oliver, K. Smettem, M. Kranz, and K. Mayer, "Field testing a wireless sensor network for reactive environmental monitoring [soil moisture measurement]," in *Proc. Int. Conf. Intell. Sensors, Sensor Netw. Inf. Process.*, Dec. 2004, pp. 7–12.
[4] A. Mainwaring, D. Culler, J. Polastre, R. Szewczyk, and J. Anderson, "Wireless sensor networks for habitat monitoring," in *Proc. 1st ACM Int. Workshop Wireless Sensor Netw. Appl.*, 2002, pp. 88–97.
[5] A. Sheth *et al.*, "SenSlide: A sensor network based landslide prediction system," in *Proc. 3rd Int. Conf. Embedded Netw. Sensor Syst.*, 2005, pp. 280–281.
[6] R. Jurdak, A. G. Ruzzelli, and G. M. P. O'Hare, "Radio sleep mode optimization in wireless sensor networks," *IEEE Trans. Mobile Comput.*, vol. 9, no. 7, pp. 955–968, Jul. 2010.
[7] *CeNSE*. [Online]. Available: http://www.hpl.hp.com/news/2009/oct-dec/cense.html
[8] L. Girod, M. Lukac, V. Trifa, and D. Estrin, "The design and implementation of a self-calibrating distributed acoustic sensing platform," in *Proc. 4th Int. Conf. Embedded Netw. Sensor Syst.*, 2006, pp. 71–84.
[9] D. Jarrell, D. Sisk, and L. Bond, "Prognostics and condition based maintenance (CBM)—A scientific crystal ball," in *Proc. 3rd Int. Congr. Adv. Nucl. Power Plants (ICAPP)*, Jun. 2002, pp. 1–8.

[10] J. P. Thomasa, M. A. Qidwai, and J. C. Kellogg, "Energy scavenging for small-scale unmanned systems," *J. Power Sour.*, vol. 159, no. 2, pp. 1494–1509, Sep. 2006.

[11] A. B. M. Alim Al Islam and V. Raghunathan, "QRTT: Stateful round trip time estimation for wireless embedded systems using *Q*-learning," *IEEE Embedded Syst. Lett.*, vol. 4, no. 4, pp. 102–105, Dec. 2012.

[12] A. B. M. A. A. Islam, M. S. Hossain, V. Raghunathan, and Y. C. Hu, "Backpacking: Deployment of heterogeneous radios in high data rate sensor networks," in *Proc. 20th Int. Conf. Comput. Commun. Netw. (ICCCN)*, Jul./Aug. 2011, pp. 1–8.

[13] F. Österlind and A. Dunkels, "Approaching the maximum 802.15.4 multi-hop throughput," in *Proc. Workshop Hot Topics Embedded Netw. Sensor Syst. (HotEmNets)*, Jun. 2008.

[14] B. Raman, K. Chebrolu, S. Bijwe, and V. Gabale, "PIP: A connection-oriented, multi-hop, multi-channel TDMA-based MAC for high throughput bulk transfer," in *Proc. 8th ACM Conf. Embedded Netw. Sensor Syst.*, 2010, pp. 15–28.

[15] R. Jurdak, K. Klues, B. Kusy, C. Richter, K. Langendoen, and M. Brunig, "Opal: A multiradio platform for high throughput wireless sensor networks," *IEEE Embedded Syst. Lett.*, vol. 3, no. 4, pp. 121–124, Dec. 2011.

[16] Y.-F. Wen, T. A. F. Anderson, and D. M. W. Powers, "On energy-efficient aggregation routing and scheduling in IEEE 802.15.4-based wireless sensor networks," *Wireless Commun. Mobile Comput.*, vol. 14, no. 2, pp. 232–253, Feb. 2014.

[17] G. Anastasi, M. Conti, M. D. Francesco, and A. Passarella, "Energy conservation in wireless sensor networks: A survey," *Ad Hoc Netw.*, vol. 7, no. 3, pp. 537–568, May 2009.

[18] S. Duquennoy, F. Österlind, and A. Dunkels, "Lossy links, low power, high throughput," in *Proc. 9th ACM Conf. Embedded Netw. Sensor Syst.*, 2011, pp. 12–25.

[19] O. Gnawali *et al.*, "The tenet architecture for tiered sensor networks," in *Proc. 4th Int. Conf. Embedded Netw. Sensor Syst.*, 2006, pp. 153–166.

[20] W. Han, "Three-tier wireless sensor network infrastructure for environmental monitoring," Ph.D. dissertation, Dept. Biol. Agricult. Eng., Kansas State Univ., Kansas, U.K., 2012.

[21] B. Kusy *et al.*, "Radio diversity for reliable communication in WSNs," in *Proc. 10th Int. Conf. Inf. Process. Sensor Netw. (IPSN)*, Apr. 2011, pp. 270–281.

[22] J. Leal, A. Cunha, M. Alves, and A. Koubaa, "On a IEEE 802.15.4/ZigBee to IEEE 802.11 gateway for the ART-WiSe architecture," in *Proc. IEEE Conf. Emerg. Technol. Factory Autom. (ETFA)*, Sep. 2007, pp. 1388–1391.

[23] N. Wang, N. Zhang, and M. Wang, "Wireless sensors in agriculture and food industry—Recent development and future perspective," *Comput. Electron. Agricult.*, vol. 50, no. 1, pp. 1–14, Jan. 2006.

[24] D. Lymberopoulos, N. B. Priyantha, M. Goraczko, and F. Zhao, "Towards energy efficient design of multi-radio platforms for wireless sensor networks," in *Proc. IPSN*, Apr. 2008, pp. 257–268.

[25] D. Lymberopoulos, N. B. Priyantha, and F. Zhao, "mPlatform: A reconfigurable architecture and efficient data sharing mechanism for modular sensor nodes," in *Proc. IPSN*, Apr. 2007, pp. 128–137.

[26] V. Raghunathan, S. Ganeriwal, and M. Srivastava, "Emerging techniques for long lived wireless sensor networks," *IEEE Commun. Mag.*, vol. 44, no. 4, pp. 108–114, 2006.

[27] D. Mclntire, K. Ho, B. Yip, A. Singh, W. Wu, and W. J. Kaiser, "The low power energy aware processing (LEAP) embedded networked sensor system," in *Proc. IPSN*, 2006, pp. 449–457.

[28] D. Jung and A. Savvides, "An energy efficiency evaluation for sensor nodes with multiple processors, radios and sensors," in *Proc. IEEE INFOCOM*, Apr. 2008, pp. 439–447.

[29] A. Capone, M. Cesana, D. D. Donno, and I. Filippini, "Deploying multiple interconnected gateways in heterogeneous wireless sensor networks: An optimization approach," *Comput. Commun.*, vol. 33, no. 10, pp. 1151–1161, Jun. 2010.

[30] C.-Y. Wan, S. B. Eisenman, A. T. Campbell, and J. Crowcroft, "Siphon: Overload traffic management using multi-radio virtual sinks in sensor networks," in *Proc. SenSys*, Nov. 2005, pp. 116–129.

[31] C. Sengul, A. Harris, T. Abdelzaher, M. Bakht, and R. Kravets, "Improving energy conservation using bulk transmission over high-power radios in sensor networks," in *Proc. ICDCS*, Jun. 2008, pp. 801–808.

[32] M. Leopold, M. B. Dydensborg, and P. Bonnet, "Bluetooth and sensor networks: A reality check," in *Proc. SenSys*, 2003, pp. 103–113.

[33] O. Boyinbode, H. Le, and M. Takizawa, "A survey on clustering algorithms for wireless sensor networks," *Int. J. Space-Based Situated Comput.*, vol. 1, no. 2, pp. 130–136, 2011.

[34] P. Kumarawadu, D. J. Dechene, M. Luccini, and A. Sauer, "Algorithms for node clustering in wireless sensor networks: A survey," in *Proc. 4th Int. Conf. Inf. Autom. Sustainability (ICIAFS)*, Dec. 2008, pp. 295–300.

[35] A. A. Abbasi and M. Younis, "A survey on clustering algorithms for wireless sensor networks," *Comput. Commun.*, vol. 30, nos. 14–15, pp. 2826–2841, 2007.

[36] S. Liu, Y. Tang, and Y. Liu, "A survey of transport protocol for wireless sensor networks," in *Proc. 2nd Int. Conf. Consum. Electron., Commun. Netw. (CECNet)*, Apr. 2012, pp. 2338–2341.

[37] A. B. M. Alim Al Islam, C. S. Hyder, H. Kabir, and M. Naznin, "Finding the optimal percentage of cluster heads from a new and complete mathematical model on LEACH," *Wireless Sensor Netw.*, vol. 2, no. 2, pp. 129–140, 2010.

[38] A. B. M. Alim Al Islam, M. S. Hossain, and V. Raghunathan, "Dynamic clustering with relay nodes (DCRN): A clustering technique to maximize stability in wireless sensor networks with relay nodes," *Int. J. Commun., Netw. Syst. Sci.*, vol. 5, no. 6, p. 368, Jun. 2012.

[39] S. Halder and A. Ghosal, "Is sensor deployment using Gaussian distribution energy balanced?" in *Algorithms and Architectures for Parallel Processing*. Berlin, Germany: Springer-Verlag, 2013, pp. 58–71.

[40] A. A. Aziz, Y. A. Sekercioglu, P. Fitzpatrick, and M. Ivanovich, "A survey on distributed topology control techniques for extending the lifetime of battery powered wireless sensor networks," *IEEE Commun. Surveys Tuts.*, vol. 15, no. 1, pp. 121–144, Feb. 2013.

[41] S. Halder and S. DasBit, "Design of a probability density function targeting energy-efficient node deployment in wireless sensor networks," *IEEE Trans. Netw. Service Manage.*, vol. 11, no. 2, pp. 204–219, Jun. 2014.

[42] *Making Large Sensor Networks Work as Real-Time Threat Assessment*. [Online]. Available: http://www.koreaittimes.com/story/16559/making-large-sensor-networks-work-real-time-threat-assessment, accessed Oct. 26, 2014.

[43] *Largest Tiny Network Yet*. [Online]. Available: http://webs.cs.berkeley.edu/800demo/, accessed Oct. 26, 2014.

[44] G. Werner-Allen, K. Lorincz, J. Johnson, J. Lees, and M. Welsh, "Fidelity and yield in a volcano monitoring sensor network," in *Proc. 7th Symp. Oper. Syst. Design Implement.*, 2006, pp. 381–396.

[45] J. Paek, N. Kothari, K. Chintalapudi, S. Rangwala, and R. Govindan, "The performance of a wireless sensor network for structural health monitoring," in *Proc. 2nd Eur. Workshop Wireless Sensor Netw.*, Istanbul, Turkey, 2005.

[46] J. Paek, K. Chintalapudi, R. Govindan, J. Caffrey, and S. Masri, "A wireless sensor network for structural health monitoring: Performance and experience," in *Proc. 2nd IEEE Workshop Embedded Netw. Sensors (EmNetS-II)*, May 2005, pp. 1–10.

[47] N. Xu *et al.*, "A wireless sensor network for structural monitoring," in *Proc. 2nd Int. Conf. Embedded Netw. Sensor Syst.*, 2004, pp. 13–24.

[48] *NetSHM—A Programmable Wireless Sensor Network for Structural Damage Detection and Localization*. [Online]. Available: http://enl.usc.edu/projects/netshm/, accessed Oct. 26, 2014.

[49] J. P. Lynch, Y. Wang, K. C. Lu, T. C. Hou, and C. H. Loh, "Post-seismic damage assessment of steel structures instrumented with self-interrogating wireless sensors," in *Proc. 8th Nat. Conf. Earthquake Eng.*, 2006, pp. 18–22.

[50] Y. Wang, J. P. Lynch, and K. H. Law, "A wireless structural health monitoring system with multithreaded sensing devices: Design and validation," *Struct. Infrastruct. Eng., Maintenance, Manage., Life-Cycle Design Perform.*, vol. 3, no. 2, pp. 103–120, 2007.

[51] S. N. Pakzad, S. Kim, G. L. Fenves, S. D. Glaser, D. E. Culler, and J. W. Demmel, "Multi-purpose wireless accelerometers for civil infrastructure monitoring," in *Proc. 5th Int. Workshop Struct. Health Monitor.*, Sep. 2005.

[52] C. Townsend and S. Arms, *Wireless Sensor Network Principles and Application*. [Online]. Available: http://www.brainwareknowledgehub.com/content/?p=599, accessed Oct. 26, 2014.

[53] L. Krishnamurthy *et al.*, "Design and deployment of industrial sensor networks: Experiences from a semiconductor plant and the north sea," in *Proc. 3rd Int. Conf. Embedded Netw. Sensor Syst.*, 2005, pp. 64–75.

[54] B. Greenstein *et al.*, "Collecting high-rate data over low-rate sensor network radios," Center Embedded Netw. Sens., Univ. California, Oakland, CA, USA, Tech. Rep. 17, 2007.

[55] J. Henaut, A. Lecointre, D. Dragomirescu, and R. Plana. (2010). "Radio interface for high data rate wireless sensor networks." [Online]. Available: http://arxiv.org/abs/1004.0204

[56] C. B. Margi, V. Petkov, K. Obraczka, and R. Manduchi, "Characterizing energy consumption in a visual sensor network testbed," in *Proc. 2nd Int. Conf. Testbeds Res. Infrastruct. Develop. Netw. Commun.*, 2006, pp. 331–339.

[57] W. Ye, J. Heidemann, and D. Estrin, "Medium access control with coordinated adaptive sleeping for wireless sensor networks," *IEEE/ACM Trans. Netw.*, vol. 12, no. 3, pp. 493–506, Jun. 2004.

[58] S.-H. Yang, H.-W. Tseng, E. H.-K. Wu, and G.-H. Chen, "Utilization based duty cycle tuning MAC protocol for wireless sensor networks," in *Proc. IEEE Global Telecommun. Conf. (GLOBECOM)*, vol. 6. Dec. 2005, pp. 3258–3262.

[59] S. Luo, X. Mao, Y. Sun, Y. Ji, and S. Tang, "Delay minimum data collection in the low-duty-cycle wireless sensor networks," in *Proc. Global Commun. Conf. (GLOBECOM)*, Dec. 2012, pp. 232–237.

[60] F. Wang and J. Liu, "On reliable broadcast in low duty-cycle wireless sensor networks," *IEEE Trans. Mobile Comput.*, vol. 11, no. 5, pp. 767–779, May 2012.

[61] T. Issariyakul and E. Hossain, *Introduction to Network Simulator NS2*. Berlin, Germany: Springer-Verlag, 2008.

[62] J. Zheng and M. J. Lee, *A Comprehensive Performance Study of IEEE 802.15. 4*. Los Alamitos, CA, USA: IEEE Press, 2004.

[63] B. Latré, P. D. Mil, I. Moerman, B. Dhoedt, P. Demeester, and N. Van Dierdonck, "Throughput and delay analysis of unslotted IEEE 802.15.4," *J. Netw.*, vol. 1, no. 1, pp. 20–28, 2006.

[64] *Energy Model Update in NS-2*. [Online]. Available: http://www.isi.edu/ilense/software/smac/ns2_energy.html, accessed Oct. 26, 2014.

[65] *Two-Ray Ground Reflection Model*. [Online]. Available: http://www.isi.edu/nsnam/ns/doc/node218.html, accessed Oct. 26, 2014.

[66] C. E. Perkins and P. Bhagwat, "Highly dynamic destination-sequenced distance-vector routing (DSDV) for mobile computers," in *Proc. SIGCOMM*, Aug. 1994, pp. 234–244.

[67] V. Chandrasekaran, "A review on hierarchical cluster based routing in wireless sensor networks," *J. Global Res. Comput. Sci.*, vol. 3, no. 2, pp. 12–16, 2012.

[68] J. Zhao and R. Govindan, "Understanding packet delivery performance in dense wireless sensor networks," in *Proc. 1st Int. Conf. Embedded Netw. Sensor Syst.*, 2003, pp. 1–13.

[69] P. Gupta and P. R. Kumar, "The capacity of wireless networks," *IEEE Trans. Inf. Theory*, vol. 46, no. 2, pp. 388–404, Mar. 2000.

[70] G. G. Messier, J. A. Hartwell, and R. J. Davies, "A sensor network cross-layer power control algorithm that incorporates multiple-access interference," *IEEE Trans. Wireless Commun.*, vol. 7, no. 8, pp. 2877–2883, Aug. 2008.

[71] K. Ozaki *et al.*, "A transmit power control algorithm for data acquisition systems," in *Proc. IEEE 75th Veh. Technol. Conf. (VTC Spring)*, May 2012, pp. 1–5.

[72] K. Ramachandran, R. Kokku, H. Zhang, and M. Gruteser, "Symphony: Synchronous two-phase rate and power control in 802.11 WLANs," in *Proc. 6th Int. Conf. Mobile Syst., Appl., Services*, 2008, pp. 132–145.

[73] M. Liu and M. T. Liu, "A power-saving algorithm combing power management and power control for multihop IEEE 802.11 ad hoc networks," *Int. J. Ad Hoc Ubiquitous Comput.*, vol. 4, nos. 3–4, pp. 168–173, 2009.

[74] S. Max and T. Wang, "Transmit power control in wireless mesh networks considered harmful," in *Proc. 2nd Int. Conf. Adv. Mesh Netw. (MESH)*, Jun. 2009, pp. 73–78.

[75] Y. W. Chung and H. Y. Hwang, "Modeling and analysis of energy conservation scheme based on duty cycling in wireless ad hoc sensor network," *Sensors*, vol. 10, no. 6, pp. 5569–5589, 2010.

[76] R. Combes, A. Proutiere, D. Yun, J. Ok, and Y. Yi. (2013). "Optimal rate sampling in 802.11 systems." [Online]. Available: http://arxiv.org/abs/1307.7309

[77] I. Pefkianakis, S. H. Y. Wong, H. Yang, S.-B. Lee, and S. Lu, "Toward history-aware robust 802.11 rate adaptation," *IEEE Trans. Mobile Comput.*, vol. 12, no. 3, pp. 502–515, Mar. 2013.

[78] Q. Pang, V. C. M. Leung, and S. C. Liew, "A rate adaptation algorithm for IEEE 802.11 WLANs based on MAC-layer loss differentiation," in *Proc. 2nd Int. Conf. Broadband Netw. (BroadNets)*, Oct. 2005, pp. 659–667.

[79] X. Chen, V. G. Subramanian, and D. J. Leith, "PHY modulation/rate control for fountain codes in 802.11a/g WLANs," *Phys. Commun.*, vol. 9, pp. 135–144, Dec. 2013.

[80] M. Lacage, M. H. Manshaei, and T. Turletti, "*IEEE 802.11* rate adaptation: A practical approach," in *Proc. 7th ACM Int. Symp. Modeling, Anal. Simulation Wireless Mobile Syst.*, 2004, pp. 126–134.

[81] S. Tang, H. Yomo, A. Hasegawa, T. Shibata, and M. Ohashi, "Joint transmit power control and rate adaptation for wireless LANs," *Wireless Pers. Commun.*, vol. 74, no. 2, pp. 469–486, Jan. 2014.

[82] K.-L. Hung and B. Bensaou, "Throughput analysis and rate control for IEEE 802.11 Wireless LAN with hidden terminals," in *Proc. 11th Int. Symp. Modeling, Anal. Simulation Wireless Mobile Syst.*, 2008, pp. 140–147.

[83] K. D. Huang, K. R. Duffy, and D. Malone, "H-RCA: 802.11 collision-aware rate control," *IEEE/ACM Trans. Netw.*, vol. 21, no. 4, pp. 1021–1034, Aug. 2013.

[84] A. B. M. Alim Al Islam and V. Raghunathan, "Assessing the viability of cross-layer modeling for asynchronous, multi-hop, ad-hoc wireless mesh networks," in *Proc. 9th ACM Int. Symp. Mobility Manage. Wireless Access*, 2011, pp. 147–152.

[85] I. Tinnirello, S. Choi, and Y. Kim, "Revisit of RTS/CTS exchange in high-speed IEEE 802.11 networks," in *Proc. 6th IEEE Int. Symp. World Wireless Mobile Multimedia Netw. (WoWMoM)*, Jun. 2005, pp. 240–248.

[86] K. Xu, M. Gerla, and S. Bae, "How effective is the IEEE 802.11 RTS/CTS handshake in ad hoc networks," in *Proc. IEEE Global Telecommun. Conf. (GLOBECOM)*, vol. 1. Nov. 2002, pp. 72–76.

[87] K. L. Addy, "Method and system for analyzing received signal strength," U.S. Patent 6 150 936, Nov. 21, 2000.

[88] W. J. Spillman and E. Lang, *The Law of Diminishing Returns*. San Diego, CA, USA: World Book Company, 1924.

[89] A. B. M. Alim Al Islam, C. Hyder, and K. H. Zubaer, "Digging the innate reliability of wireless networks," in *Proc. Int. Conf. Netw. Syst. Secur. (NSysS)*, to be published.

[90] B. He, B. Xie, and D. P. Agrawal, "Optimizing deployment of internet gateway in wireless mesh networks," *Comput. Commun.*, vol. 31, no. 7, pp. 1259–1275, May 2008.

[91] J. Luo, W. Wu, and M. Yang, "Optimization of gateway deployment with load balancing and interference minimization in wireless mesh networks," *J. UCS*, vol. 17, no. 14, pp. 2064–2083, 2011.

[92] J. L. Wong, R. Jafari, and M. Potkonjak, "Gateway placement for latency and energy efficient data aggregation [wireless sensor networks]," in *Proc. 29th Annu. IEEE Int. Conf. Local Comput. Netw.*, Nov. 2004, pp. 490–497.

[93] S. Ibrahim, M. Al-Bzoor, J. Liu, R. Ammar, S. Rajasekaran, and J.-H. Cui, "General optimization framework for surface gateway deployment problem in underwater sensor networks," *EURASIP J. Wireless Commun. Netw.*, vol. 2013, no. 1, pp. 1–13, 2013.

[94] X. Liu and P. Mahapatra, "On the deployment of wireless sensor nodes," in *Proc. 3rd Int. Workshop Meas., Modeling, Perform. Anal. Wireless Sensor Netw. (SenMetrics)*, Jul. 2005, pp. 78–85.

[95] H. Zhang and C. Liu, "A review on node deployment of wireless sensor network," *Int. J. Comput. Sci. Issues*, vol. 9, no. 6, pp. 1–6, Nov. 2012.

[96] M. O. Farooq and T. Kunz, "Wireless sensor networks testbeds and state-of-the-art multimedia sensor nodes," *Appl. Math. Inf. Sci*, vol. 8, no. 3, pp. 935–940, 2014.

[97] P. Levis *et al.*, "TinyOS: An operating system for sensor networks," in *Ambient Intelligence*. Berlin, Germany: Springer-Verlag, 2005, pp. 115–148.

[98] G. Coley, "Beagleboard system reference manual," *BeagleBoard*, p. 81, Dec. 2009.

[99] *DM3730, DM3725 Digital Media Processors*. [Online]. Available: http://www.ti.com.cn/cn/lit/ds/symlink/dm3730.pdf, accessed Oct. 26, 2014.

[100] *Mini Wireless N USB Adapter*. [Online]. Available: http://www.trendnet.com/products/proddetail.asp?prod=190_TEW-648UB, accessed Oct. 26, 2014.

[101] D. Moss, J. Hui, and K. Klues, "Low power listening," in *Proc. Core Working Group, TEP*, vol. 105, 2007.

[102] T. McConnel. (2009). *WIRELESS/RF: SenSiFi WiFi Sensor Module Promises Battery Life of 3+ Years*, http://www.eetimes.com/document.asp?doc_id=1311688

[103] A. B. M. Alim Al Islam, C. S. Hyder, H. Kabir, and M. Naznin, "Stable sensor network (SSN): A dynamic clustering technique for maximizing stability in wireless sensor networks," *Wireless Sensor Netw.*, vol. 2, no. 7, pp. 538–554, Jul. 2010.

[104] *IRIS Datasheet*. [Online]. Available: http://www.nr2.ufpr.br/~adc/documentos/iris_datasheet.pdf, accessed Oct. 26, 2014.

[105] *Micaz Datasheet*. [Online]. Available: http://www.openautomation.net/uploadsproductos/micaz_datasheet.pdf, accessed Oct. 26, 2014.
[106] J. Zhang, P. V. Orlik, Z. Sahinoglu, A. F. Molisch, and P. Kinney, "UWB systems for wireless sensor networks," *Proc. IEEE*, vol. 97, no. 2, pp. 313–331, Feb. 2009.
[107] S. Gezici *et al.*, "Localization via ultra-wideband radios: A look at positioning aspects for future sensor networks," *IEEE Signal Process. Mag.*, vol. 22, no. 4, pp. 70–84, Jul. 2005.
[108] M. B. Nejad, "Ultra wideband impulse radio for wireless sensing and identification," Ph.D. dissertation, KTH, Stockholm, Sweden, 2008.
[109] L. L. Peterson and B. S. Davie, *Computer Networks: A Systems Approach*. San Francisco, CA, USA: Morgan Kaufmann, 2007.
[110] F. J. Richards, "A flexible growth function for empirical use," *J. Experim. Botany*, vol. 10, no. 2, pp. 290–301, 1959.
[111] R. S. Michalski, J. G. Carbonell, and T. M. Mitchell, *Machine Learning: An Artificial Intelligence Approach*, vol. 1. San Mateo, CA, USA: Morgan Kaufmann, 1985.
[112] J. Jin, A. Sridharan, B. Krishnamachari, and M. Palaniswami, "Handling inelastic traffic in wireless sensor networks," *IEEE J. Sel. Areas Commun.*, vol. 28, no. 7, pp. 1105–1115, Sep. 2010.
[113] S. Eswaran, M. P. Johnson, A. Misra, and T. L. Porta, "Distributed utility-based rate adaptation protocols for prioritized, quasi-elastic flows," *ACM SIGMOBILE Mobile Comput. Commun. Rev.*, vol. 13, no. 1, pp. 2–13, 2009.

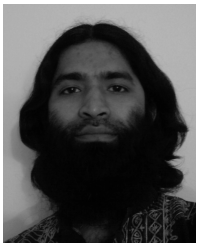

A. B. M. ALIM AL ISLAM received the B.Sc. (Eng.) and M.Sc. (Eng.) degrees in computer science and engineering from the Department of Computer Science and Engineering, Bangladesh University of Engineering and Technology (BUET), Dhaka, Bangladesh, in 2006 and 2009, respectively, and the Ph.D. degree in computer engineering from the School of Electrical and Computer Engineering, Purdue University, West Lafayette, IN, USA, in 2012.

He is currently serving as an Assistant Professor with the Department of Computer Science and Engineering, BUET, where he served as a Lecturer from 2007 to 2013. He served as a member of the Department of Research and Development in Commlink InfoTech Ltd., Dhaka, Bangladesh, and Stochastic Logic, ACI, Dhaka, from 2006 to 2007 and in 2006, respectively. His research interests cover wireless mesh networking, wireless sensor networking, multiradio networks, network protocols, near-field communication, modeling and simulation, and reliability analysis. He has co-authored several journal and conference papers, and presented his papers in different well-reputed venues. He served on Organizing and Technical Program Committees of several conferences and workshops.

Dr. Islam was a recipient of the Andrew's Fellowship, and a Two-Year Prestigious Fellowship from the School of Electrical and Computer Engineering, Purdue University. In addition, he received several other awards, such as the Dean's Award from the Faculty of Electrical and Electronics Engineering, BUET, the Academic Merit Scholarship from the Department of Computer Science and Engineering, BUET, and general scholarships from the Rajshahi Board, Bangladesh. He also received several awards for the best paper, best poster, best demo, and best project.

MOHAMMAD SAJJAD HOSSAIN received the B.Sc. (Eng.) degrees in computer science and engineering from the Department of Computer Science and Engineering, Bangladesh University of Engineering and Technology (BUET), Dhaka, Bangladesh, in 2004, the M.Sc. degree in computer science from Stony Brook University, Stony Brook, NY, USA, in 2008, and the Ph.D. degree in computer engineering from the School of Electrical and Computer Engineering, Purdue University, West Lafayette, IN, USA, in 2011.

He is currently serving with Google Inc., Mountain View, CA, USA. His research interests cover software architectures for networked embedded systems, and distributed and cloud computing. He has co-authored several journal and conference papers, and presented his papers in different well-reputed venues.

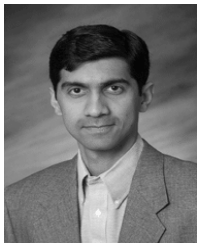

VIJAY RAGHUNATHAN received the B.Tech. degree from IIT Madras, Chennai, India, in 2000, and the M.S. and Ph.D. degrees from the University of California at Los Angeles (UCLA), Los Angeles, CA, USA, in 2002 and 2006, respectively, all in electrical engineering.

He is currently an Associate Professor in the School of Electrical and Computer Engineering at Purdue University, West Lafayette, IN, USA, where he leads the Embedded Systems Laboratory. He was a Visiting Researcher with NEC Laboratories America, Princeton, NJ, USA, from 2005 to 2006. His research interests include hardware and software architectures for embedded computing systems, system-on-chip design, and wireless sensor networks, with an emphasis on low-power design, microscale energy harvesting, and reliable system design. He has co-authored two book chapters, several journal and conference papers, and has presented full-day and embedded tutorials on the above topics. He serves on the Organizing and Technical Program Committees of several leading ACM and IEEE conferences in the areas of embedded systems, very large scale integration design, and sensor networks. In 2011, he served as the Technical Program Co-Chair of the ACM/IEEE International Conference on Information Processing in Sensor Networks.

Dr. Raghunathan was a recipient of the NSF CAREER Award, the Edward K. Rice Outstanding Doctoral Student Award from the School of Engineering and Applied Sciences, UCLA, and the Outstanding Masters Student Award from the Department of Electrical Engineering, UCLA. He was also a recipient of the Best Paper Award at the ACM International Conference on Embedded Networked Sensor Systems in 2011, the Design Contest Award at the ACM/IEEE International Symposium on Low Power Electronics and Design (ISLPED) in 2005, the Best Student Paper Award at the IEEE International Conference on VLSI Design in 2000, and the Best Paper Award Nomination at the ACM/IEEE ISLPED in 2006.

YU CHARLIE HU (S'91–M'03–SM'07) received the B.S. degree in computer science from the University of Science and Technology of China, Hefei, China, the M.S. and M.Phil. degrees in computer science from Yale University, New Haven, CT, USA, in 1989 and 1992, respectively, and the Ph.D. degree in computer science from Harvard University, Cambridge, MA, USA, in 1997.

He is currently serving as a Professor with the School of Electrical and Computer Engineering, Purdue University, West Lafayette, IN, USA. Prior to joining Purdue University in 2002, he was a Research Scientist with the Systems Group, Department of Computer Science, Rice University, Houston, TX, USA. He was a Visiting Researcher with Microsoft Research Redmond, Redmond, WA, USA, in Fall 2008.

Prof. Hu's research interests are in mobile, distributed systems, operating systems, networking, and high-performance computing. He leads the Distributed Systems and Networking Laboratory at Purdue University, where he is also a member of the Center for Wireless Systems and Applications. He co-founded the International Workshop on Mobile Peer-to-Peer Computing series in 2004. He was a recipient of the Honda Initiation Grant Award in 2002, the NSF CAREER Award in 2003, and the Purdue University College of Engineering Early Career Research Award in 2009. He was named as an ACM Distinguished Scientist in 2010.